

Hydroclimatic processes as the primary drivers of the Early Khvalynian transgression of the Caspian Sea: new developments

Alexander Gelfan^{1,2}, Andrey Panin^{1,3}, Andrey Kalugin¹, Polina Morozova³,

Vladimir Semenov^{1,3,4}, Alexey Sidorchuk², Vadim Ukraintsev^{1,3}, Konstantin Ushakov^{1,5}

¹ Water Problems Institute, Russian Academy of Sciences, Moscow, 119333, Russia

² Lomonosov Moscow State University, Faculty of Geography, Moscow, 119991, Russia

³ Institute of Geography, Russian Academy of Sciences, Moscow, 119017, Russia

⁴ Obukhov Institute of Atmospheric Physics, Russian Academy of Sciences, 119017 Moscow, Russia

⁵ Shirshov Institute of Oceanology, Russian Academy of Sciences, 117997 Moscow, Russia

Correspondence to: Alexander Gelfan (hydrowpi@mail.ru)

Abstract. It has been well established that during the late Quaternary, the Khvalynian transgression of the Caspian Sea occurred, when the sea level rose tens of meters above the present one. Here, we evaluate the physical feasibility of the hypothesis that the maximum phase of this extraordinary event (known as the “Early Khvalynian transgression”) could be initiated and maintained for several thousand years solely by hydroclimatic factors. The hypothesis is based on recent studies dating the highest sea level stage (well above +10 m a.s.l.) to the final period of deglaciation, 17-13 kyr BP, and studies estimating the contribution of the glacial waters in the sea level rise for this period as negligible. To evaluate the hypothesis put forward, we first applied the coupled ocean and sea-ice general circulation model driven by the climate model and estimated the equilibrium water inflow (irrespective of its origin) sufficient to maintain the sea level at the well-dated marks of the Early Khvalynian transgression as 400-470 km³/year. Secondly, we conducted an extensive radiocarbon dating of the large paleochannels (signs of high flow of atmospheric origin) located in the Volga basin and found that the period of their origin (17.5-14 ka BP) is almost identical to the recent dating of the main phase of the Early Khvalynian transgression. Water flow that could form these palaeochannels was earlier estimated for the ancient Volga River as 420 km³/year, i.e., close to the equilibrium runoff we determined. Thirdly, we applied a hydrological model forced by paleoclimate data to reveal physically consistent mechanisms of an extraordinarily high water inflow into the Caspian Sea in the absence of a visible glacial meltwater effect. We found that the inflow could be caused by the spread of post-glacial permafrost in the Volga paleo-catchment. The numerical experiments demonstrated that the permafrost resulted in a sharp drop in infiltration into the frozen ground and reduced evaporation, which all together generated the Volga runoff during the Oldest Dryas, 17-14.8 kyr BP, up to 360 km³/year (i.e., the total inflow into the Caspian Sea could reach 450 km³/year). The closeness of the estimates of river inflow into the sea, obtained by three independent methods, in combination with the previously obtained results, gave us reason to conclude that the hypothesis put forward is physically consistent.

1 Introduction

Paleogeographical data give grounds to assert that during the late Quaternary the largest highstand in the Quaternary history of the Caspian Sea took place, which was called the "Great" Khvalynian transgression. The boundaries of the Khvalynian Sea are well-detected in the relief of the Northern Caspian lowland (e.g. Leontiev, 1968, 1977; Rychagov, 1974, 1997), and confirmed by stratigraphic and biostratigraphic analysis of Quaternary deposits (Fedorov, 1957, 1978; Svitoch and Yanina, 1997; Svitoch, 2009, 2014; Yanina, 2012; Makshaev and Svitoch, 2016; Yanina et al.,

39 2018; Kurbanov et al., 2021). The accumulated data show that in the early, maximum stage of the Khvalynian
40 transgression, the sea level rose up to +48 m a.s.l., i.e. almost 80 meters above the current Caspian Sea level (CSL),
41 while the sea surface area was 940,000 km², which is 2.5 times larger than its current area (Yanko-Hombach and
42 Kislov, 2018). After the maximum level was reached, there was a breakthrough of the Caspian into the Manych
43 Depression, which caused a westward flow into the Black Sea (Svitoch et al., 2010; Semikolennykh et al., 2022).

44 Although the very fact of the Early Khvalynian transgression and the assessment of the maximum sea level are not
45 questioned by most researchers, there are significant disagreements regarding the dating of this extraordinary
46 hydrological phenomenon and the views on its genesis.

47 Before the 1990s, most researchers believed that the maximum phase of the Khvalynian transgression was
48 synchronous to the Early Valdai (Early Weichselian, MIS 4) glaciation of the Russian Plain and occurred 50-70 ka
49 BP (see reviews by Kislov et al., 2014; Arslanov et al., 2016 and references there). Nevertheless, the first radiocarbon
50 (¹⁴C) dating data allowed already in the early 1970s to formulate the idea of a younger age of this transgression, dating
51 to the very end of the Late Pleistocene (Kaplin et al., 1972, 1973; Svitoch and Parunin, 1973; Svitoch and Yanina,
52 1983). The accumulation of geochronometric, mostly ¹⁴C, data is increasingly argued in favor of a younger age of the
53 Early Khvalynian transgression, corresponding to the second half of the last glaciation (Late Valdai, Late Weichselian,
54 MIS 2) (Svitoch et al., 1994, 1998; Svitoch and Yanina, 1997). A number of compilations of the accumulated
55 geochronological data have been published in recent years that enable a more detailed interpretation of the
56 transgression. Arslanov et al. (2016) summarized the ¹⁴C and ²³⁰Th/²³⁴U dates of the Lower Khvalynian deposits and
57 proposed to date the +35 and +22 m a.s.l. transgressive stages at 16 and 14 ka BP, respectively, while the period 14-
58 12 ka BP was attributed to stages 0 and -12 m a.s.l. of the subsequent Late Khvalynian transgression. Krijgsman et al.
59 (2019), based on a review of available dates, assigned the entire Khvalynian epoch to the 35-10 ka BP interval, with
60 the Yenotayevka regression separating the Early and Late Khvalynian phases, about 15 ka BP. Koriche et al. (2022)
61 attributed the Early Khvalynian stage to 35-25 ka BP and the Late Khvalynian stage to 17-12 ka BP. The latter,
62 according to (Koriche et al., 2022), reached +35 m a.s.l. during 14.5-16.5 ka BP. Makshaev and Tkach (2023), based
63 on a generalization of 234 ¹⁴C dates, of which elevation data were available for 182 dates, attributed the Early
64 Khvalynian stage of the Caspian Sea to the period 36-12.5 ka BP. In their opinion, sea level exceeded the contemporary
65 level at the beginning of MIS 2 (28-25 ka BP). This was followed by two highstands at 25-18 ka BP (level reached
66 +10+15 m a.s.l.) and 17-13.5 ka BP (+20+22 m a.s.l.), separated by a sea level drop between 18 and 17 ka BP. These
67 authors date the Yenotayevka regression and the subsequent Late Khvalynian transgression to 12.5-8.5 ka BP.

68 Recently, a series of papers have been published where sections containing the Khvalynian sediments were first dated
69 by optically stimulated luminescence (OSL) (Kurbanov et al., 2021, 2022, 2023; Butuzova et al., 2022; Taratunina et
70 al., 2022). These results were summarized in Kurbanov et al. (2023), who identified the following transgression stages:
71 1) sea level rise to about +5 m a.s.l (32 m above the present CSL) between 30-35 and 27 ka BP; 2) sea level stabilization
72 with a slight (about 2 m) rise within the interval of 27-20 ka BP; 3) a sharp rise in the sea level beginning from 18-17
73 ka BP; 4) maximum stage of the sea level during the period around 16-15 ka BP; 5) rapid fall of the sea level during
74 the period 15-14 ka BP from its maximum values to less than +11 m a.s.l.

75 Thus, the Khvalynian stage in the development of the Caspian Sea can currently be referred to the period from the end
76 of MIS 3 (about 35 ka BP) to the Early Holocene (8.5 ka BP). At the beginning of that period, the sea level was lower
77 than it is now, but no later than 27 ka BP it was already much higher. It should be emphasized that no direct dates for
78 the maximum stage of +48+50 m a.s.l. have been obtained in any study. The recently published OSL data on the

79 Raygorod section in the Northern Caspian Lowland at +13.5 m a.s.l. (Taratunina et al., 2022) show that from at least
80 90 ka BP up to 18 ka BP, subaerial deposits (alluvium, loess) were accumulating there, i.e., the maximum phase of
81 transgression could not have occurred before the Last Glacial Maximum (LGM). The age of the maximum stage is
82 best justified by (Kurbanov et al., 2023), where the maximum stage is sandwiched between the rise and fall phases
83 and is assigned to the interval of 15-16 ka BP. Therefore, taking into account the reliable recent dating reviewed above,
84 we will limit our attempt to explain the genesis of the Early Khvalynian transgression to the final period of
85 deglaciation, (18)17-13 kyr BP.

86 Another widely debated question is: what are the causes of the Early Khvalynian transgression? The discussed
87 hypotheses are reduced to the consideration of the sources of a huge water influx into the sea, which, under the climatic
88 conditions of the Late Pleistocene, could provide the sea level rise of tens of meters above the present CSL. Other
89 causes, such as tectonic factors or natural, internal fluctuations of the water body, are considered unlikely (Rychagov,
90 1997; Yanko-Hombach and Kislov, 2018, respectively). According to paleoclimatic modeling experiments (e.g.
91 Kislov and Toropov, 2007; Morozova, 2014; Yanko-Hombach and Kislov, 2018; Morozova et al., 2021), the LGM
92 and post-LGM climate is characterized by low air temperatures and low precipitation with a reduced, relative to the
93 modern, climatic runoff, that is, the difference between precipitation and evaporation in the catchment area of the
94 Caspian Sea. To explain the increased river inflow into the Caspian Sea as a factor of the Early Khvalynian
95 transgression, hypotheses are put forward about additional, in comparison with atmospheric precipitation, sources of
96 water. The most discussed hypothesis is the recharge of glacial meltwater from the south-eastern flank of the
97 Scandinavian ice sheet (SIS) via the Volga River during the LGM and deglaciation (Kvasov, 1979; Varuschenko et
98 al., 1987; Toropov and Morozova, 2011; Tudryn et al., 2016; Koriche et al., 2022). Hypotheses are also put forward
99 about the overflow of glacially dammed lakes and water discharge from outside the drainage basin of the Caspian Sea
100 - from the upper Dnieper catchment and from the Sukhona and Vychegda Rivers that belong to the Arctic Ocean
101 catchment (Kvasov, 1979; Larsen et al., 2006; Lyså et al., 2011), from the Aral Sea basin through a hypothetical
102 hydrological system connecting it with both the ice-dammed lakes of the West Siberian ice-sheet and the Caspian Sea
103 (see Grosswald and Kotlyakov, 1989; Chepalyga, 2007, as well as a critique of this hypothesis by Svitoch (2009) and
104 Panin et al. (2020)). Kvasov (1979) estimated the contribution of the SIS meltwater and proglacial lakes as 46% and
105 input from the Aral Sea as 21% of the total water inflow into the Early Khvalynian Caspian Sea, which was estimated
106 by this author as 560 km³/year. Based on the PMIP2 (Paleoclimate Modelling Intercomparison Project, Phase 2)
107 climate simulation data, Toropov and Morozova (2011) estimated that the SIS meltwater could have made the main
108 contribution to the Khvalynian transgressions: 83% of the ancient Volga River inflow assessed as 462 km³/year. The
109 coupled atmosphere-ocean-vegetation HadCM3 climate model experiments allowed Koriche et al. (2022) to conclude
110 that meltwater combined with the changes (due to isostatic adjustment) in the drainage system leading to an increase
111 in the Caspian Sea catchment area by 60-70% of its modern size, had the most substantial influence on the sea level
112 rise during the last deglaciation from 20 kyr BP to 14 kyr BP. Note that all the above estimates of the SIS meltwater
113 contribution were obtained solely from modelling results, which were not confirmed by geological and/or
114 geomorphological evidence.

115 The validity of the above hypotheses considering glacial meltwater as a substantial source of water inflow into the
116 Caspian Sea and confidence in the corresponding estimates of meltwater contribution to the Early Khvalynian
117 transgression, are directly related to the assessed age of the transgression. According to the present-day state of
118 geochronological studies described above, the stages well above +10 m a.s.l. are dated to the period of (18)17-13 kyr
119 BP. Tudryn et al. (2016) proposed that glacial meltwater entered the Caspian Sea during the entire deglaciation epoch

120 up to 13.8 kyr BP. However, Panin et al. (2021) showed that the inflow of meltwater into the Volga basin occurred
121 only from its upper part directly covered by the Scandinavian ice-sheet, and was limited to a period from 21 to 16.5
122 kyr BP, i.e. the transgression was developing towards its highest stage, while the input of glacial waters ceased. The
123 authors estimated the possible glacial meltwater input to the upper Volga River in the range of 15-70 km³/year, or
124 only 5–25% of the present-day Volga runoff into the Caspian Sea, which is far from enough to support the Khvalynian
125 highstand. The insignificant role of glacial meltwater in the genesis of the Early Khvalynian transgression during the
126 deglaciation period is also argued in earlier works (Kalinin et al, 1966; Panin et al., 2005; Sidorchuk et al., 2009).
127 Also, a number of recent studies (Panin et al., 2020, 2022; Borisova et al., 2022) showed that neither the proglacial
128 lakes in the upper Volga region proposed by Kvasov (1979), nor the overflow to the Volga River from the Arctic basin
129 occurred in MIS 2.

130 The hypothesis of hydroclimatic initiation of the Early Khvalynian transgression, in the absence of a noticeable
131 contribution from glacial meltwater, is supported by the ubiquitous presence in the southern half of the Eastern
132 European Plain, including the Volga basin, of signs of high flow of atmospheric origin - river palaeochannels that are
133 many times greater in size than the contemporary rivers (Sidorchuk et al., 2009, 2011, 2021; Ukraintsev, 2022). On
134 the basis of the developed morphometric analysis of palaeochannels, Sidorchuk et al. (2009, 2021) estimated the
135 meteoric (formed due to atmospheric precipitation) runoff of the ancient Volga River, which was capable of forming
136 the palaeochannels, as 420 km³/year, i.e. 65% higher than the modern annual runoff. At physically reasonable ratios
137 of precipitation and evaporation in the Caspian Sea, this is quite sufficient to maintain levels of the Early Khvalynian
138 transgression (Sidorchuk et al., 2009; Kislov et al., 2014).

139 The age of large palaeochannels in the Dnieper, Don, and Volga basins obtained by the ¹⁴C method falls within the
140 interval of 18-13 kyr BP (Borisova et al., 2006; Sidorchuk et al., 2009; Panin et al., 2013, 2017; Panin and Matlakhova,
141 2015), that is, exactly at the time when the CSL rose above +10 m a.s.l. However, it should be noted that in the Volga
142 basin itself, only two large palaeochannels have been dated so far on the Moskva River, a tributary of the Oka River,
143 and on the Samara River, a tributary of the lower Volga (Sidorchuk et al., 2009). This is insufficient for such a large
144 basin encompassing several natural zones with significant differences in the present climate. In this study, we clarified
145 the period of activity of large palaeochannels in the Volga basin.

146 Thus, according to the above review there is a knowledge gap, which drives the main motivation for our study. On
147 the one hand, the well-founded modern datings show that in the final period of deglaciation, 18(17)-13 kyr BP, the
148 CSL rose well above +10 m a.s.l. (likely, up to +22 ÷ +35 m a.s.l.), but, on the other hand, it has been proved that the
149 meltwater runoff – due to the Scandinavian ice-sheet melting and outbursts of ice-dammed proglacial lakes - was
150 either absent or contributed insignificantly to the transgression of the sea during this period. A research question arises:
151 could the Early Khvalynian transgression of the Caspian Sea have been initiated and maintained solely by
152 hydroclimatic factors in the cryoarid climate of the deglaciation period and in the absence of an inflow of glacial
153 meltwater?

154 Kislov and Toropov (2007), Sidorchuk et al. (2009) hypothesized that during the decline in the glacier melt, river flow
155 into the sea could significantly exceed the current one due to the spread of post-glacial permafrost in the river
156 catchments of the East European Plain. Permafrost could reduce evaporation for the sea catchment territory owing to
157 a drastic decrease in the infiltration capacity of frozen ground. Gelfan and Kalugin (2021) applied a physically based
158 hydrological model to assess the sensitivity of the Volga River runoff to the hypothetical spread of permafrost in the
159 river basin. The authors demonstrated that under the modern climatic conditions mean annual runoff may increase by
160 85% due to modeled "freezing" of the basin. They concluded that river inflow into the Caspian Sea is markedly

161 sensitive to presence of permafrost over the sea catchment area, thus further verification of the hypothesis is advisable
162 in the cryoarid climatic conditions of the late Pleistocene. One of the objectives of our study is to verify this hypothesis
163 explaining the maintenance of the CSL at +22 ÷ +35 m a.s.l. reliably dated to the period of 18(17)-13 kyr BP in the
164 absence of significant glacial meltwater runoff during this period.

165 The logic of our study was as follows. Using a full ocean model coupled with a model of sea-ice dynamics INMIO
166 COMPASS – CICE (Ibrayev et al., 2012; Hunke et al., 2015), we simulated the Caspian Sea water balance
167 components under the climate conditions of the Late Pleistocene – Middle Holocene, which were re-constructed with
168 the help of the climate model INMCM4.8 (Volodin et al., 2018). On the basis of the simulation data, we estimated the
169 equilibrium river water inflow into the sea maintaining its level at the well-dated marks of the Early Khvalynian
170 transgression. To verify the model-based estimations, the river runoff assessments derived from the morphometry of
171 palaeochannels formed in the period 18-13 kyr BP (Sidorchuk et al., 2021) were used. Also, we made an attempt to
172 improve the knowledge on the chronology of widespread geomorphological evidence of high river runoff in the Late
173 Pleniglacial – Late Glacial in the Volga basin. To achieve this, additional dating of large palaeochannels in different
174 parts of the basin was carried out. Then, the hydrological model was forced by the paleoclimate data, and numerical
175 experiments were conducted to assess the water inflow to the Caspian Sea from the ancient Volga catchment with
176 underlying permafrost. Comparison of estimates of water inflow into the Caspian Sea obtained using three independent
177 approaches (1 – estimating equilibrium inflow into the sea via an ocean model coupled with a climate model; 2 -
178 paleogeographic reconstructions of water flow through palaeochannels, and 3 – hydrological modeling river runoff
179 generation in the sea catchment area under the paleoclimatic conditions) provided us with grounds for answering the
180 above research question.

181 The remaining part of this paper is organized as follows. General information about the Caspian Sea is given in the
182 next section. Section 3 contains methodology of our study including brief description of the models used and the
183 numerical experiments designed. The results are presented and discussed in Section 4. The overall conclusions are
184 given in Section 5.

185 **2. General information on the Caspian Sea**

186 The Caspian Sea (36°33'–47°07' N, 46°43'–54°50' E) is the world's largest inland water body located within an
187 endorheic (no outflow) basin. The sea surface area at the current sea level is equal to 365,000 km². The coastline
188 length is 5970 km. The greatest length of the sea (along the meridian 50°00'E) is 1030 km. The greatest width along
189 the parallel 45°30' N reaches 435 km. The large meridional extent results in climate variations over the basin: from
190 sub-tropical in the southwest to desertic in the east and northeast.

191 Owing to the endorheic nature of the Caspian Sea, its level widely fluctuated in the past. During the late Cenozoic,
192 the CSL variations exceeded, probably, several hundreds of meters (Forte and Cowgill, 2013) and at least 100 m,
193 during the last 500,000–700,000 years (Water balance..., 2016), during the Holocene the CSL changes were from 15
194 m (Water balance..., 2016) to several tens of meters (Kakroodi et al., 2012), during the last millennium the CSL
195 changed by 10 m (Naderi Beni et al., 2013) and during the period of instrumental observations (beginning from 1830)
196 within the range of 4 m: from -25.1 m a.s.l. at the beginning of 1880s to -29.0 m a.s.l. in the middle of 1970s (Frolov,
197 2003). The present (November of 2023) CSL is -29.1 m a.s.l.

198 The CSL variations are controlled mainly by water inflow from rivers and precipitation on the sea, as well as by water
199 outflow through evaporation from the sea surface (Ratkovich, 1993; Golitsyn et al., 1998; Kroonenberg et al., 2000;

200 Arpe and Leroy, 2007; Arpe et al., 2012; Naderi Beni et al., 2013; Panin and Dianskii, 2014; Chen et al., 2017), i.e.
201 they are strongly dependent on climatic variations (Kroonenberg et al., 2000; Arpe and Leroy, 2007;), at least as long
202 as no significant changes are occurring in the sea catchment area. Groundwater inflow contribution is estimated to be
203 small (Zektser, 1996) and expected to partly compensate for the impact from the outflow to the Kara-Bogaz-Gol Bay
204 (Chen et al., 2017) accounting for the uncertainty of both estimates.

205 The Caspian Sea is fed by more than 130 large and small rivers with the total annual flow of about 300 km³ (average
206 value for 1880-2001 (Frolov, 2003)). The total catchment area of the sea is 3,050,000 km², which is 8 times the area
207 of its water area (386,400 km² at the sea level of -27.50 m a.s.l.). The largest of the tributaries is the Volga River,
208 whose catchment area is 1,360,000 km². For the period of instrumental observations (1881-2012), the mean annual
209 flow of the Volga in the river outlet (Volgograd city) is about 250 km³ (e.g. Arpe et al., 2019). Taking into account
210 water losses due to evaporation in the Volga delta, the Volga water inflow into the Caspian Sea is about 233 km³ of
211 water per year (Frolov, 2003) or about 80% of the total inflow of river water into the sea. According to (Kislov and
212 Toropov, 2007), the relative contribution of the Volga runoff has changed insignificantly over the past 20 thousand
213 years and accounts for 75 to 90% of the total inflow into the Caspian Sea. According to various estimates, the long-
214 term mean precipitation on the Caspian Sea surface in the 20th century was about 200 mm/year (about 77 km³/year),
215 evaporation from the sea surface was 960 mm/year (about 371 km³/year), and effective evaporation (the difference
216 between evaporation and precipitation) was 760 mm/year (about 294 km³/year), respectively (Frolov, 2003; Water
217 Balance..., 2016).

218 The relationship between water input to and output from the Caspian Sea controls the sea level. The CSL response to
219 changes in the main water balance components of the sea depends on the peculiarities of the sea bathymetry, namely,
220 a significant fraction of shallow water areas. The northern part of the sea is shallow, in the southern and central parts
221 of the sea there are deep depressions that are intersected by an underwater ridge. The average depth of the sea is 208
222 m, the maximum depth is 1025 m. About 69% of the total sea area is at depths less than 200 meters, and a shallow
223 zone with depths less than 10 m occupies 28% of the sea area. In the range of the CSL fluctuations from -28.0 to -
224 24.0 m a.s.l., a one-meter change in the CSL results in a 1500 km² change in the area of the deep-water part of the sea,
225 and a 12500 km² change in the area of the shallow-water North Caspian part (Frolov, 2021). The predominant increase
226 in the water area due to the shallow waters of the Northern Caspian with a rise in the sea level creates a non-linear
227 dependence of evaporation from sea level fluctuations (Frolov, 2003).

228

229 **3 Research Methods**

230 **3.1 Hydro- thermodynamics model of the Caspian Sea**

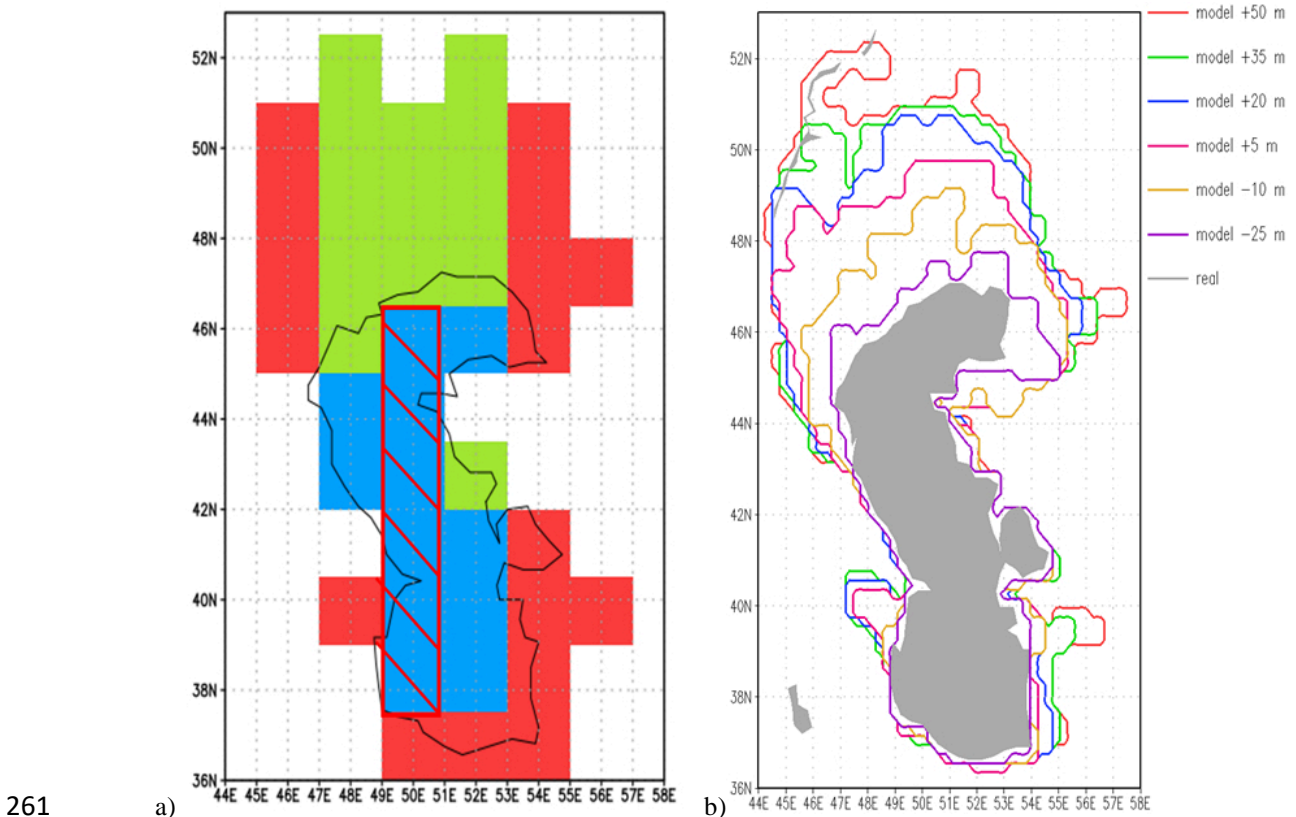
231 To simulate the Caspian Sea water balance components, we used a regional configuration of the coupled ocean and
232 sea-ice general circulation model INMIO COMPASS – CICE (Ibrayev et al., 2012; Hunke et al., 2015). This approach
233 involves a detailed description of marine dynamic processes with a high spatiotemporal resolution, taking into account
234 ice drift and energy-mass transfer in the water-ice-atmosphere system. Thus, it is possible to obtain more reasonable
235 values of evaporation from the sea surface compared to global climate models, in which a coarser resolution is
236 typically used and the sea level is set constant, allowing no change in the surface area when the water balance of the
237 sea is different from zero. The importance of using a full ocean model for the Caspian Sea was demonstrated by (Arpe
238 et al., 2019).

239 The coupled model built from INMIO COMPASS (Ibrayev et al., 2012) and CICE (Hunke et al., 2015) codes in the
 240 CMF2.0 software environment (Kalmykov et al., 2018) was used earlier for weather forecasting and climate research
 241 (Fadeev et al., 2018; Kalnitskii et al., 2020; Ushakov and Ibrayev, 2018, and references therein). The model solves
 242 the equations of three-dimensional dynamics and thermodynamics of the ocean and sea ice cover, explicitly
 243 reproducing a wide range of processes responsible for the main energy-carrying elements of the circulation. The
 244 calculations were performed using a model configuration tuned for the Caspian Sea region with a spatial resolution of
 245 about 22 km and a time step of 20 minutes, which was described in (Morozova et al., 2021).

246 3.2 Assessing equilibrium river inflow into the paleo-Caspian Sea under the transgressive levels of the sea

247 To assess an equilibrium river inflow into the paleo-Caspian Sea, the paleo-climate data simulated by the INMCM4.8
 248 climate model (Volodin et al., 2018) were set as atmospheric boundary conditions for the coupled ocean-ice model
 249 according to the protocols of PMIP4 (Paleoclimate Modelling Intercomparison Project, Phase 4) and CMIP6 (Coupled
 250 Model Intercomparison Project, Phase 6). The paleo-climate data represent two periods: the Last Glacial Maximum
 251 (experiment LGM, 21 kyr BP, Kageyma et al., 2021) and the mid-Holocene (experiment midHolocene, 6 kyr BP,
 252 Brierley et al., 2020). The data included near-surface air temperature and specific humidity, precipitation, wind
 253 velocity vector, fluxes of incoming longwave and shortwave radiation. The time resolution of the boundary fields was
 254 6 hours, which made it possible to explicitly consider a wide range of variability, from synoptic to interannual scales.

255 Since the Caspian Sea in the experiments of the climate model was specified in the modern coastline, the isolines of
 256 some boundary fields (air temperature and humidity, incoming longwave radiation) showed a tendency to follow this
 257 coastline. For these fields, an extrapolation was made from the sea area domain adopted by the climate model to the
 258 area of transgression. Since the sea level rise affects mainly the northern coastal regions, the extrapolation was
 259 performed from south to north using the meridional gradients calculated for each field by the least square method over
 260 the central part of the climate model water area (Fig. 1a).



262 **Figure 1: a) The Caspian Sea area representation in the climate model INMCM4.8 (blue cells), red shading - cells used to**
 263 **calculate meridional gradients, green and red cells - extrapolation areas for transgressive stages (green cells – meridional**
 264 **extrapolation, red cells – extrapolation by the nearest neighbor method); b) The model representation of the Caspian Sea**
 265 **coastline for the sea levels assigned in the numerical experiments. The grey fill shows modern boundaries of the sea.**
 266

267 Further, for several transgressive cells, where this meridional procedure is not applicable, a simple extrapolation by
 268 the nearest neighbor method was performed. Precipitation, wind velocity components, and incoming shortwave
 269 radiation were used directly without extrapolation.

270 Calculations of the water balance in the LGM and mid-Holocene were carried out for a range of the CSL: from the
 271 near-modern one (-25 m a.s.l.) to the maximum level of the Early Khvalynian transgression (+50 m a.s.l.), with a step
 272 of 15 meters, a total of six experiments. The corresponding model domains are shown in Fig. 1b.

273 For each of the two paleo-periods and each sea level, the experiment was performed for 50 model years and was
 274 organized as follows (Table 1). First, a rough initial approximation for the annual mean river runoff was specified as
 275 a linear function of the sea area (Morozova et al., 2021). After that, a model spin-up was performed for five years, and
 276 then during the next 15 years of model integration the average water imbalance was calculated. At the end of the 20th
 277 year, the obtained average imbalance was subtracted from the river runoff, and the average anomaly was subtracted
 278 from the sea level field. This resulted in the equilibrium runoff value and reinitialized sea level, which were used to
 279 further proceed with the calculations. Another spin-up was performed for 10 years, and finally, the last 20 years of the
 280 experiment were used to analyze the fields of evaporation and precipitation over the sea.

281

282 **Table 1 – Stages of numerical experiments with the coupled ocean-ice model**

Years	Experiment stage
1 – 5	Initial approximation for the runoff. Spin-up.
6 – 20	Initial approximation for the runoff. Calculating water imbalance.
end of year 20	Applying corrections to runoff and sea level
21 – 30	Corrected runoff. Spin-up.
31 – 50	Corrected runoff. Analyzing the Caspian Sea water balance components

283 **3.3 Investigating the chronology of large palaeochannels**

284 Dating was carried out by the radiocarbon (¹⁴C) method in the laboratories of the Institute of Earth Sciences, St.
 285 Petersburg University (index LU) and the Institute of Geography, Russian Academy of Sciences, Moscow (index
 286 IGRAN). Plant remains and dispersed organic matter in gyttja were used for dating. Fresh water mollusk shells, which
 287 are frequently met in drill cores, were not used because of the high probability of date distortion due to the hard water
 288 effect. Boring for organics sampling was carried out by a mechanical corer, usually in the centre of the palaeochannel
 289 (depending on its accessibility for the machine). The geological structure of the palaeochannels usually distinguishes
 290 3-4 sedimentary units, from top to bottom: (1) overbank alluvia - silty loam, sandy loam, or peat in place of the filled
 291 up oxbow lake; (2) oxbow lake sediments - clayey loam; (3) sediments of the intermediated stage of the palaeochannel
 292 abandonment, when it was not yet completely isolated from the river and flow still continued; usually silty sand or
 293 sandy silts; (4) channel alluvium - sands, sands with gravel and pebbles. Below the bed of channel alluvium
 294 corresponding to the studied palaeochannel, there were often older alluvial deposits, which could be of diverse
 295 composition - sands, loams, gyttja (unit 5).

296 Samples from channel alluvium (unit 4) are preferred for dating as they correspond to the time of active palaeochannel
297 development. However, the channel alluvium is well-washed and organic inclusions are rare. They are much more
298 commonly found in unit 3 sediments. The process of gradual abandonment of channel meanders usually takes a few
299 years, at the most a few decades. This is less than the usual interval of uncertainty of ^{14}C dates and from the point of
300 view of geological time can be considered as a moment. Therefore, we considered that the samples from unit 4 also
301 belong to the time of active development of the palaeochannels, its very end. Unfortunately, in unit 4, as well as in
302 unit 5, organic materials suitable for dating were found only in a small number of boreholes. They were much more
303 common in unit 2. As oxbow lakes in palaeochannels could have existed for a long time (millennia), samples were
304 taken only from the very bottom of unit 3, and when interpreting the dates obtained, it was taken into consideration
305 that they refer to the time when the active development of the palaeochannels ceased. In addition, in some cases, it
306 was possible to sample for ^{14}C from unit 5, the ancient alluvium underlying the channel alluvium of the palaeochannel
307 under study. Such dates were interpreted as predating the time of activity of the studied palaeochannel.

308 Thus, in terms of the stratigraphic position, the dates have been divided into three groups:

- 309 • dates from units 3, 4, giving the time of activity of large palaeochannels - activity dates;
- 310 • dates from unit 2, referring to the time when the studied palaeochannels had already been abandoned - post-
311 dates;
- 312 • dates from unit 5, indicating the time when the large palaeochannels were not yet active - pre-dates.

313 In order to determine the total activity interval of large palaeochannels in the Volga basin within each of the groups,
314 the dates were summarised. For this purpose, the OxCal 4.4 software Sum module (Bronk Ramsey, 2009) was used.

315 **3.4 Modeling water inflow into the Caspian Sea from the ancient Volga catchment covered by permafrost**

316 Numerical experiments were carried out with a physically based model of runoff generation in the Volga River basin
317 (Motovilov, 2016; Kalugin, 2022) developed on the basis of the ECOMAG hydrological modeling platform
318 (Motovilov et al., 1999). Earlier, Gelfan and Kalugin (2021) applied the ECOMAG-based model of the Volga basin
319 for assessing the river runoff sensitivity to the hypothetical permafrost distribution over the basin area.

320 The model describes spatially variable processes of snow accumulation and snowmelt, heat and water transfer within
321 the vegetation-soil system, evapotranspiration, infiltration into frozen and unfrozen soil, soil freezing and thawing,
322 surface, subsurface and groundwater flow into the river network, and river channel flow with a daily time-step. The
323 model inputs include spatially distributed daily precipitation, air temperature and air humidity data. The Volga River
324 basin was schematized onto grid cells with a mean area of 1750 km².

325 A detailed description of the ECOMAG-based Volga River model, methods for setting the parameters and model
326 verification results for the modern climate were presented by Gelfan and Kalugin (2021). In particular, it was shown
327 that the developed model is robust against climate changes, i.e. it allows one to obtain stable (in statistical sense)
328 results of hydrological simulations within the Volga River basin for years with contrasting climatic conditions. We
329 consider the robustness of the hydrological model as a necessary condition for its applicability for paleohydrological
330 reconstructions.

331 As the boundary conditions in our experiments, we used climate data simulated by the MPI-ESM-CR global climate
332 model, which reproduced climate conditions of the deglaciation period (26-0 kyr BP) with prescribed ice sheets and
333 surface topographies from ICE-6G reconstruction (Peltier et al., 2015) within the framework of PMIP4 experiment

334 (Kapsch et al., 2021). The used climate data included monthly series of the near ground meteorological data obtained
335 within a transit experiment Ice6G_P2 (Kapsch et al., 2021) for the last 26,000 years with a hundred-year averaging
336 period. The MPI-ESM-CR model has a spatial resolution of 3.75° in longitude and 3.7° in latitude on average.

337 For hydrological modeling, we applied climate simulation data for the four following periods: the post-LGM (18-17.1
338 kyr BP), the Oldest Dryas (17-14.8 kyr BP), the Bølling (14.7-14.1 kyr BP) and the Allerød (14-12.8 kyr BP). Since
339 a hydrological model requires daily data, the monthly MPI-ESM-CR-simulated data were transformed into the series
340 of the corresponding daily values by the delta-change temporary downscaling method (Gelfan et al., 2017). For the
341 transformation, we used daily data of the meteorological observations for the period of 1985-2014 at 306
342 meteorological stations located within the Volga River basin. As a result, we constructed 30-year artificial time-series
343 of daily precipitation, air temperature and air humidity, so that their mean values were equal to the corresponding
344 long-term means calculated from monthly series for each of the four considered paleo-periods. The constructed series
345 were assigned as the boundary conditions for the hydrological model.

346 Taking into account that the climatic boundaries of permafrost follow approximately with an isotherm of the mean
347 annual air temperature below -5° C (Smith, Riseborough, 2002), in our experiments, the presence of permafrost was
348 assumed if the climatic data demonstrated a drop in the mean annual air temperature in the Volga basin below -5° C,
349 i.e. by about 10°C less than the mean air temperature in the modern climate (+4.5°C). For all elements of the
350 computational domain underlain by permafrost, the initial temperature of soils was set as negative from the ground
351 surface to the depth of 3 meter (the depth of attenuation of the seasonal temperature fluctuations).

352 The hydrological model also took into account the features of the vegetation cover in the considered paleoperiods.
353 Simakova (2008) and Makshaev (2019) showed that during the post-LGM and the Oldest Dryas, periglacial tundra
354 landscapes were common in the ancient Volga basin. The model parameters corresponding to these landscapes were
355 set using the Global Land Cover Characterization database (Loveland et al., 2000).

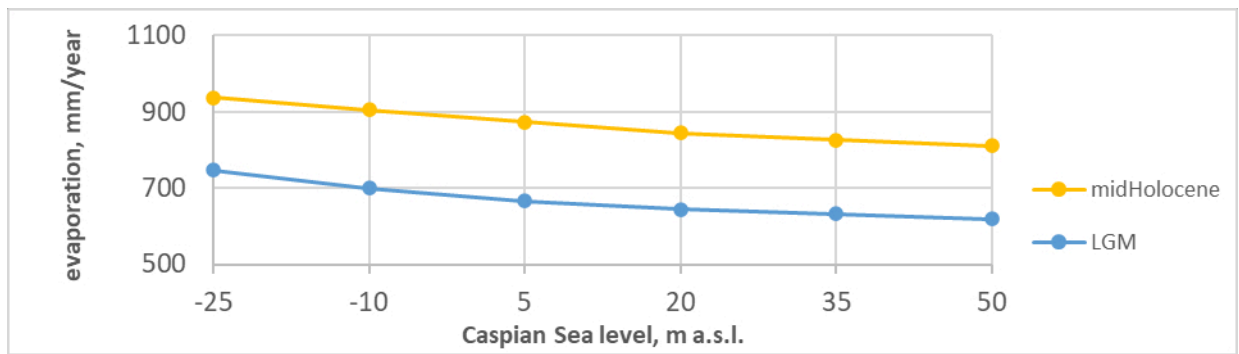
356 **4. Results and Discussion**

357 **4.1 Estimates of equilibrium river runoff to the Caspian Sea at the Early Khvalynyan transgression levels**

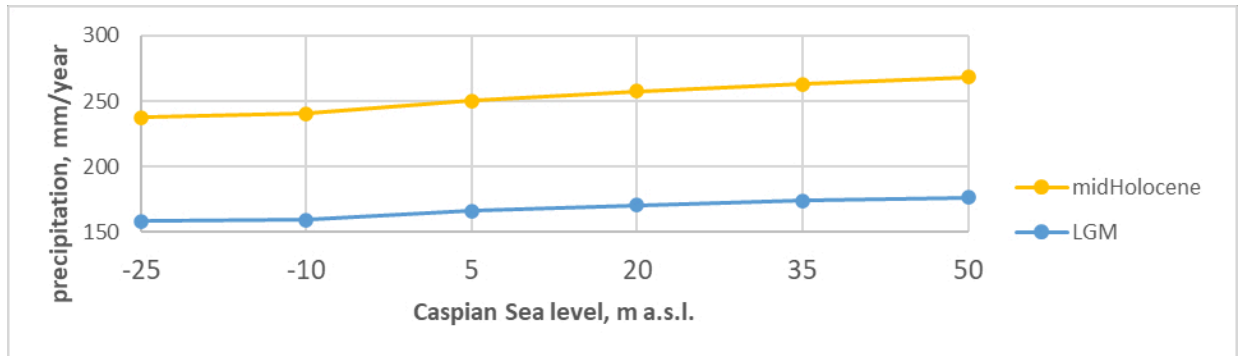
358 The numerical simulations with the INMIO COMPASS - CICE model (Sec. 3.2) provided estimates of the Caspian
359 Sea water balance components for a wide range of possible CSLs under climatic conditions of the Last Glacial
360 Maximum and the Holocene Climatic Optimum. Fig. 2 shows the average simulated values of evaporation and
361 precipitation (mm/year) over the Caspian Sea surface area, as well as the river runoff volume (km³/year) required to
362 maintain different prescribed CSLs at equilibrium conditions.

363

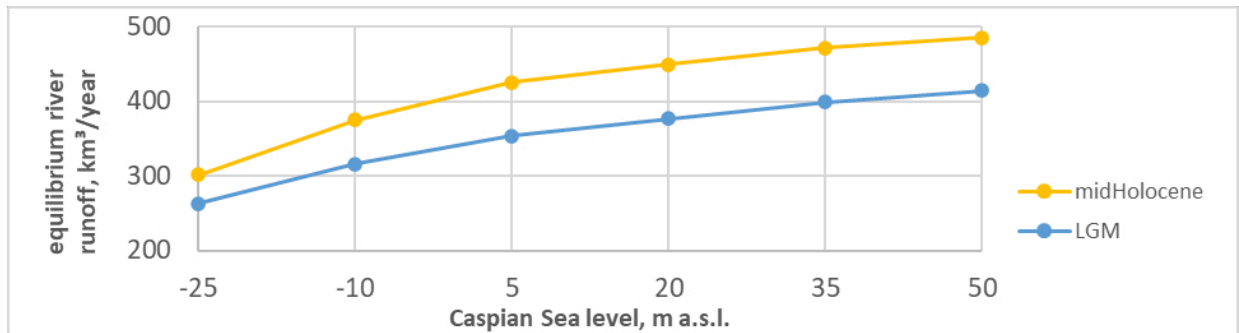
364



365



366



367

368 **Figure 2: Simulated Caspian Sea water balance components for different transgressive states under climatic conditions of**
 369 **the Last Glacial Maximum and the Holocene Climatic Optimum: averaged over the sea area evaporation (a), precipitation**
 370 **(b), and equilibrium river runoff (c) as a function of the sea level.**
 371

372 As can be seen from Fig. 2, the average evaporation decreases when the CSL rises. This is related to the peculiarities
 373 of the Caspian Sea morphology: under the CSL rise, the coastline expands predominantly in the northern direction,
 374 where temperatures are lower, and the sea ice cover period is longer. Precipitation, on the contrary, slightly increases,
 375 but this growth does not compensate for the decrease in evaporation, so the average values of effective evaporation
 376 for the entire Caspian Sea surface area also decrease with the rising sea level above -25 m a.s.l. In general, the change
 377 in the equilibrium runoff is proportional to the change in the Caspian Sea surface area, but this dependence is not
 378 linear. For the CSL above -25 m a.s.l., the Caspian Sea expands to the northern flat shore and the increase in the sea
 379 area accelerates.

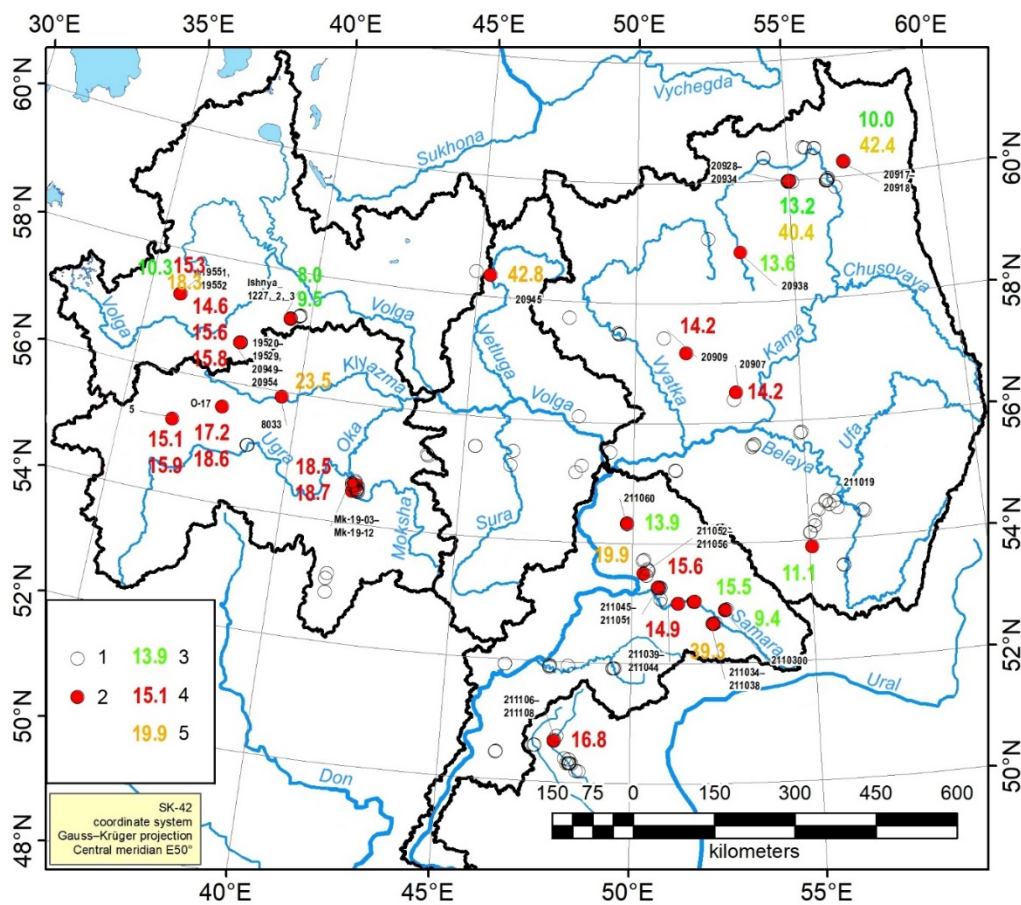
380 This is accompanied by a decrease in the river discharge increment per unit area increase. For the level range of -25
 381 ÷ -10 m a.s.l., this increment is 0.55 km³/year per 10³ km² for mid-Holocene conditions, and 0.40 km³/year per 10³
 382 km² for LGM. For the transgressive +35 ÷ +50 m a.s.l. range, however, it becomes 0.25 km³/year per 10³ km² for both
 383 mid-Holocene and LGM. Under LGM conditions, both evaporation and precipitation over the sea surface area are
 384 much lower than the corresponding values during mid-Holocene. Simulated evaporation is on average 180-200
 385 mm/year lower, and precipitation is 70-90 mm/year lower, which results in 15-20% lower values of the equilibrium
 386 runoff in LGM compared to mid-Holocene conditions for the CSLs above -25 m a.s.l.

387 Given lower air temperatures during LGM and a large shallow water area in the north at transgressive states of the
 388 Caspian Sea, the sea ice cover extent and duration play a major role in the decrease in evaporation from the sea surface.
 389 Model simulations suggest that the evaporation changes are affected by sea ice export to the warmer southern part of
 390 the Sea driven by sea circulation and surface winds. This effect is important not only during the spring melting season,
 391 but also in winter on the marginal freezing part of the water area, where the sea ice is thin.

392 The chosen LGM and mid-Holocene periods presumably represent the most contrasting climatic conditions during
 393 the late Pleistocene-early Holocene, so we interpreted the simulated values of the equilibrium river runoff as a possible
 394 range of changes during the deglaciation period under consideration. According to our results, the river runoff values
 395 required to sustain the CSL at the highest dated transgressive state at +35 m a.s.l. (17-13 kyr BP) belong to the range
 396 of 400-470 km³/year. Assuming that the contribution of the Volga River runoff to the total river discharge in that
 397 period was close to the modern one (about 80%), we estimated the river runoff from in the Volga watershed during
 398 the period of the Early Khvalynian transgression ((18)17-13 kyr BP) as 320-375 km³/year, i.e. 1.3-1.5 times larger
 399 than the present day's values.

400 4.2 Results of dating large palaeochannels in the Volga basin

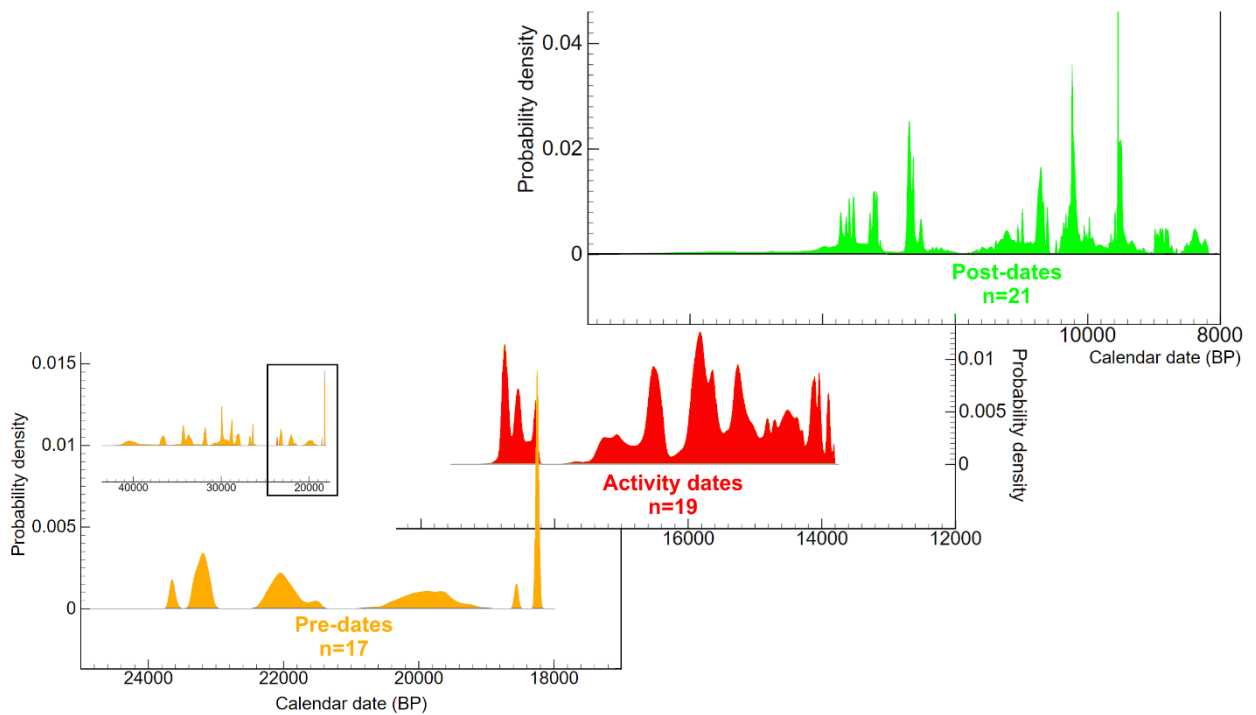
401 Drilling of large palaeochannels in different parts of the Volga basin was carried out and ¹⁴C dates were obtained for
 402 a part of the boreholes (Fig. 3). A total of 57 dates suitable for statistical analysis of the palaeochannel activity time
 403 were obtained. Dates were received from the valleys of 18 rivers: Dubna, Medveditsa, Ustyia (upper Volga basin),
 404 Moskva, Protva, Moksha (Oka basin), upper Kama, Izh, Kilmez, Lolog, Yazva, Dema (Kama basin), Samara, Sok,
 405 Buzuluk, B. Cheremshan, B. Kinel (lower Volga basin), B. Uzen (Northern Pre-Caspian).



406

407 **Figure 3: Map of cores made in large palaeochannels over the Volga basin (1 – all cores, 2 – dated cores; type of dates: 3 –**
408 **post-dates, 4 – activity dates, 5 – pre-dates. Numbers are central points of ¹⁴C calibrated dates).**
409

410 All dates are divided into three groups - 19 activity dates, 21 post-dates and 17 pre-dates (see the Methods section)
411 and for each group the summation was done in OxCal 4.4 (Fig. 4). The resulting distributions suggest the following.
412 The direct dates in the channel alluvium of the large palaeochannels form two clusters, the main one between 13.8-
413 17.3 ka BP and a small complementary one between 18.2-18.8 ka BP. The latter overlaps with the youngest part of
414 the distribution of dates in the underlying sediments (pre-dates), from which we can conclude that, with a high
415 probability, there is no generation of palaeochannels of the corresponding age. This cluster of dates may be related to
416 the dating of redeposited ancient organics.



417 **Figure 4: Summed distributions of radiocarbon dates from large palaeochannels in river valleys of the Volga basin.**
418
419

420 On the right, the distribution of dates in the fluvial alluvium is clearly limited to dates in the overlying sediments
421 (post-dates). It should be noted that in the interval of 12.5-13.8 ka BP, the dates for the overlying sediments are derived
422 from the bottoms of the palaeochannel fills (those cases where there was no material suitable for dating in the channel
423 alluvium). However, at present one can only say with certainty that the stage of large palaeochannel formation and
424 the corresponding epoch of high river runoff in the Volga basin lasted from at least 17.5 to 14 ka BP. A visual analysis
425 of the map (Fig. 3) shows no regional differences in dates, i.e. the epoch started and ended geologically simultaneously
426 in the whole Volga basin. Attention is drawn to the gap in the dates in the interval from 12.5 to 11.5 ka BP
427 corresponding to the Younger Dryas epoch and the very beginning of the Holocene. This may be a result of a shortage
428 of organic material due to scarcity of vegetation during this harsh epoch, but more likely reflects low fluvial activity
429 and a significant drop in river flow in general.

430 The determined interval of activity of big palaeochannels shows that from at least 17.5 to 14 ka BP the Volga River
431 runoff considerably exceeded the modern one. This corresponds generally to the palaeoclimate estimates from
432 paleofloristic data by Borisova (2021) who established a significant increase in atmospheric precipitation in the central
433 East European Plain in the second half of MIS 2 during the warming events 17–19 ka BP (the Late Pleniglacial) and

434 13–14.5 ka BP (the Bølling and Allerød interstadials). The Oldest Dryas cooling at 14.5–17 ka BP was characterized
435 by a decrease in precipitation below the present-day values, but the high runoff coefficients due to the existence of
436 permafrost could have favored still high runoff values. These estimates point that during the aforementioned period
437 of big palaeochannel activity, the flow hardly remained constant, but it cannot be determined by geomorphological
438 methods: among large palaeochannels there are no distinctive age generations that would differ consistently in size.
439 All large palaeochannels make up a single set of forms, clearly differing in size and position in the valley floor
440 topography from younger palaeochannels, the sizes of which correspond to modern rivers. The distribution of dates
441 for the large palaeochannels also does not reveal clear periodicity or discontinuity on the basis of which the internal
442 periodicity of the high flow epoch could be judged. Perhaps the available number of dates is not yet sufficient for this.
443 At this stage we can only mark the time frames of the epoch of high river discharge, which began no later than 17.5
444 ka BP and ended no earlier than 14 ka BP, and relate the estimate of the annual Volga runoff magnitude obtained from
445 the size of the palaeochannels (420 km³ (Sidorchuk et al., 2021)) to this epoch as a whole. Probably the drop of activity
446 dates at around 16 ka (Fig. 4) marks the Oldest Dryas pause in high river flow and big channel formation, but to
447 establish it reliably a much larger massif of dates is necessary.

448 The interval of increased inflow of river water into the Caspian Sea from 17.5 to 14 ka BP corresponds exactly to the
449 main phase of the Early Khvalynian transgression dated by marine sediments in the Northern Caspian Lowland from
450 18-17 to 14-13 ka BP (see the review in the Introduction). It was shown in section 4.1 that such amount of the Volga
451 runoff, 420 km³, was more than enough to keep the Caspian level at +35 m a.s.l. - the highest dated shoreline of the
452 Khvalynian transgression (remember that the considered maximum level of +48 ÷ +50 m a.s.l. has not yet been
453 characterized by any direct date - see the review in the Introduction).

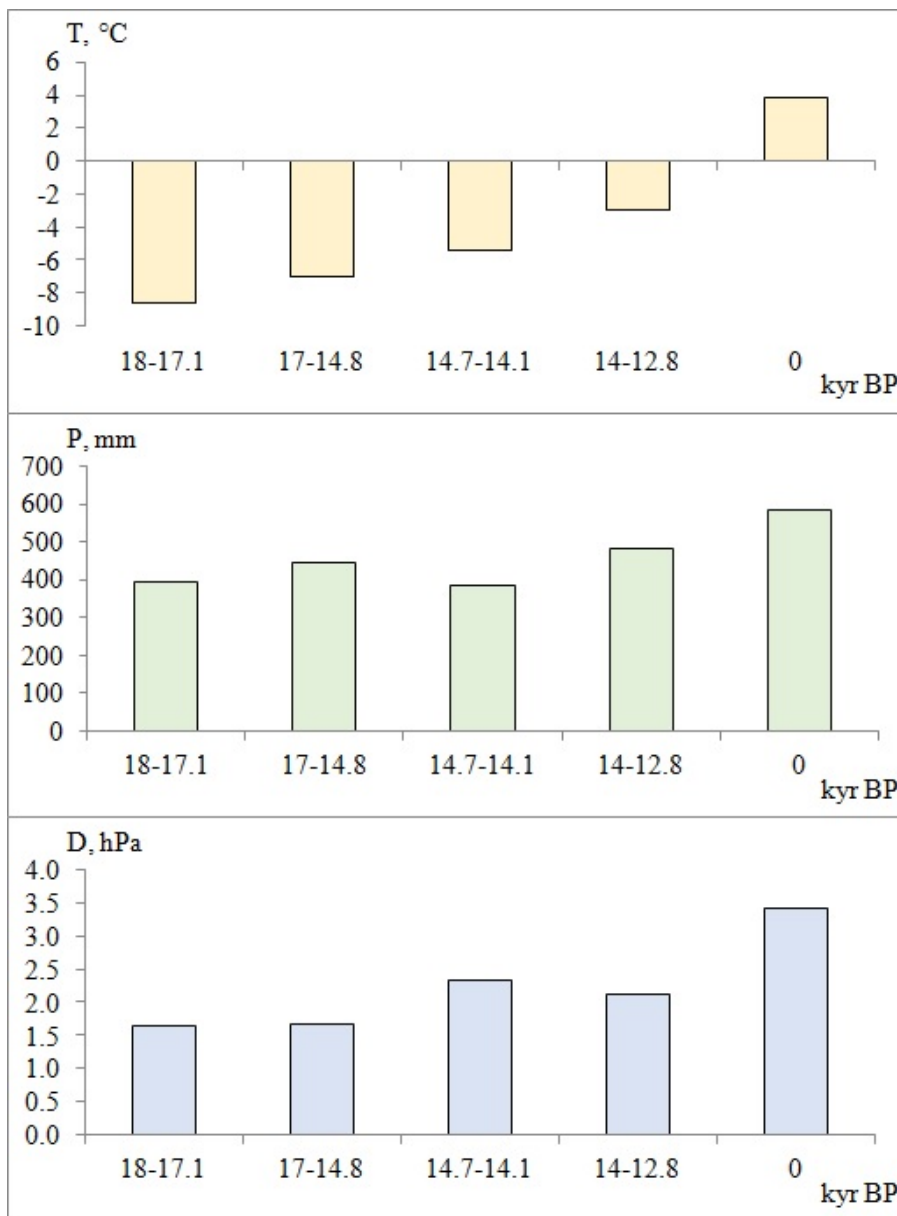
454 What could be the reasons for such a significant increase in river runoff? The involvement of glacial meltwater is
455 excluded because large palaeochannels are present in various parts of the Volga basin, including those completely
456 isolated not only from the last, but also from all Quaternary glaciations in general (for example, basins of the lower
457 Volga or right tributaries of the Oka). It is easy to show that possible increase in river runoff due to thawing of
458 permafrost, which undoubtedly took place after the LGM, was also negligible. Let us assume that water exchange
459 between groundwater and river water covered the upper 100 m of the Earth's crust. Let us also assume that during the
460 last glacial epoch, this entire stratum had a deliberately overestimated ice content of 50%, and the deliberately
461 unfeasible condition that all meltwater entered the river network when the permafrost melted. It is not difficult to
462 calculate that if this 100-meter layer of permafrost had melted during the above 3,000-year period, it would have
463 increased the annual river runoff from the modern basin area by less than 23 km³, which is less than 10% of the
464 average modern flow volume in the Volga basin. It should be emphasized that this estimate is repeatedly
465 overestimated. In reality, the additional inflow of water due to melting permafrost could be an order of magnitude
466 less.

467 Thus, huge water flowing into the Caspian Sea from the Volga basin during the period from 17 to 13 ka BP could only
468 be of atmospheric origin (except for possible minor glacial meltwater runoff from the sources of the Volga itself at
469 the very beginning of this period as demonstrated by Panin et al. (2021)). As mentioned in the Introduction, Gelfan
470 and Kalugin (2021) quantified a significant decrease in runoff losses due to the hypothetical spread of permanently
471 frozen soils over the Volga catchment and the resulting increase in the runoff coefficient, i.e. proportion of
472 precipitation involved in the river runoff formation. But the question arises: is the amount of precipitation
473 corresponding to the cryoarid climate of the deglaciation epoch enough to form an extraordinary river runoff even
474 with the spread of permafrost over the catchment area of the Caspian Sea? To answer this question, we carried out

475 numerical experiments with a hydrological model that reproduce the formation of river inflow into the Caspian Sea in
476 the climatic conditions of the period from 17 to 13 ka BP and under the assumption of frozen catchment area of the
477 sea. The results are presented in the next section.

478 4.3 Modeling the Volga River runoff in the climate conditions from the post-LGM to the Allerød (18-13 kyr 479 BP)

480 Fig. 5 illustrates changes in the mean annual precipitation, air temperature and air humidity deficit assessed from the
481 MPI-ESM-CR-simulated monthly data and averaged over the Volga basin for four periods: the post-LGM (18-17.1
482 kyr BP), the Oldest Dryas(17-14.8 kyr BP), the Bølling (14.7-14.1 kyr BP) and the Allerød (14-12.8 kyr BP), covering
483 the epoch of the Early Khvalynian transgression.



484
485 **Figure 5: MPI-ESM-CR-simulated data of the mean annual air temperature, total precipitation and air humidity deficit,**
486 **averaged over the Volga basin, during the considered periods of paleo-time and under the modern climate.**
487

488 According to these data, all considered periods were colder than the modern climate in the Volga River basin, herewith
489 each subsequent period was warmer than the previous one. Mean annual precipitation values assessed for different
490 periods were 18-34% less than the modern value. Due to the cold climate, all the periods are characterized by an

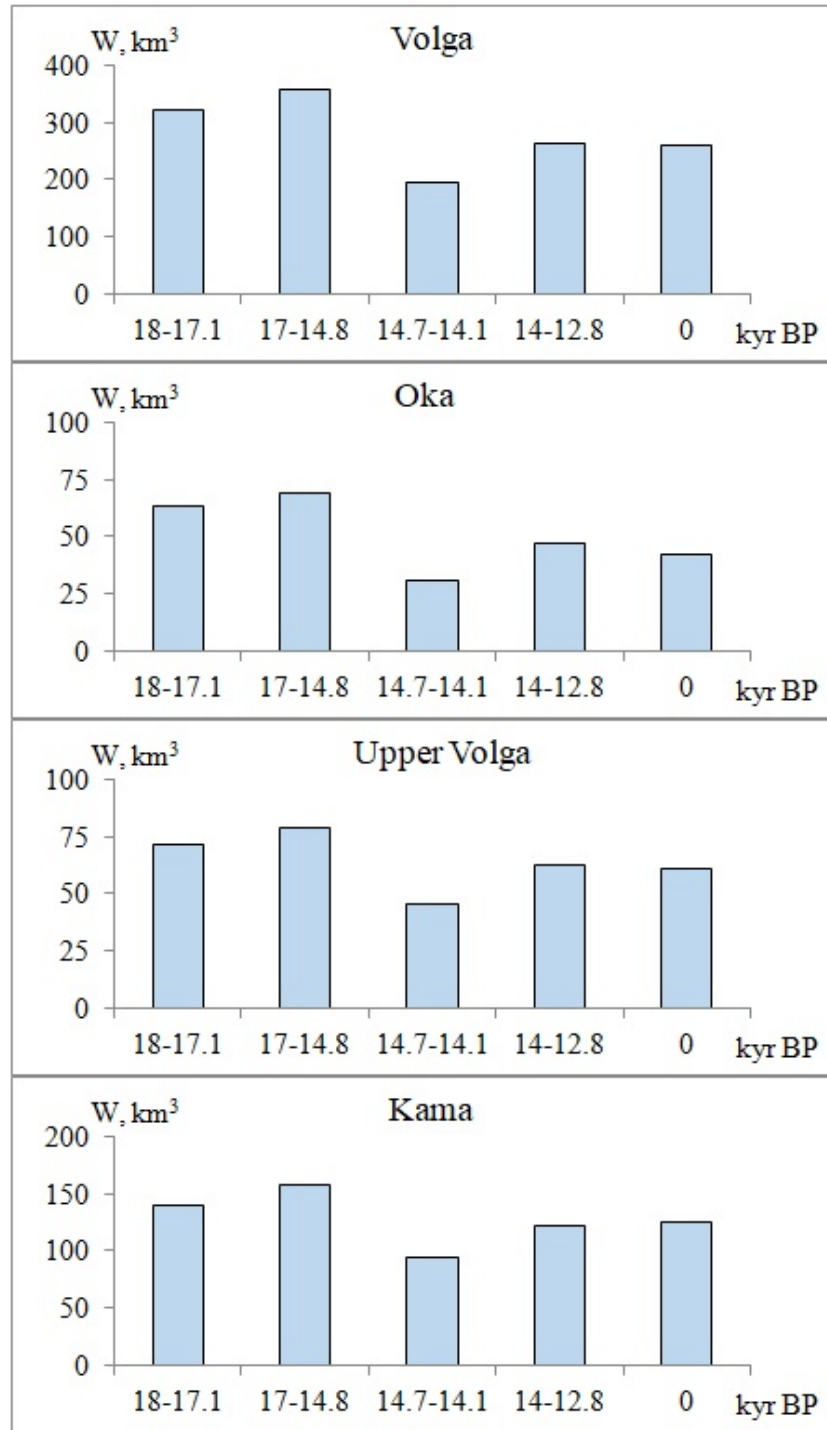
491 increase in the mean annual solid precipitation from 7% in the post-LGM and the Bølling to 41% in the Allerød
492 (relative to the modern values). On the contrary, the mean annual liquid precipitation sum decreased from 45% in the
493 Oldest Dryas to 54% in the Bølling. The mean annual air humidity deficit, which affects evaporation from the
494 catchment surface, turned out to be lower than the modern one by an average of 40-50% in different periods.

495 Taking into account the cold climate in the post-LGM period, when the average annual temperature was 12.6°C lower
496 than the present one (see Fig. 5), the Oldest Dryas (10.9°C lower) and the Bølling (9.4°C lower), we assumed that the
497 whole catchment area was covered by continuous permafrost during these three periods. Generally, this assumption
498 corresponds to the paleogeographic findings of Sidorchuk et al. (2008) and Borisova (2021). An algorithm that allows
499 taking into account the hypothetical presence of permanently frozen ground in the Volga River catchment and
500 modeling the hydrological effect of permafrost was described by Gelfan and Kalugin (2021).

501 Numerical experiments with the hydrological model, which was forced by the temporary downscaled paleo-climate
502 data, demonstrated that the mean annual runoff of the ancient Volga during the post-LGM period and the Oldest Dryas
503 increased in comparison with the modern one for the period of 1985-2014 (259 km³) by 24% and 38%, respectively
504 (Fig. 6). The runoff rising during the Oldest Dryas was larger due to larger mean precipitation. The permafrost led to
505 a decrease in the infiltration capacity of the soils by more than an order of magnitude in comparison with the unfrozen
506 soil over the river catchment. Decreased soil infiltration resulted in an increase in the mean runoff coefficient to as
507 much as 0.67, i.e. 2/3 of precipitation falling on the catchment was not lost and reached the river channels and then
508 the Caspian Sea (note that the mean annual runoff coefficient in the modern climate for the Volga basin is 0.35, i.e.
509 almost twice as low). As a result, the assessed permafrost-induced changes in the runoff coefficient could themselves
510 lead to an increase in the mean runoff even with a decrease in the mean precipitation comparing with the modern one.
511 And this growth became especially noticeable due to the reduced evaporation from the catchment area caused by the
512 decrease in the air humidity deficit during the post-LGM period and the Oldest Dryas (Fig. 5). At the same time, the
513 mean runoff visibly dropped during the Bølling period in spite of the permafrost presence that can be explained by a
514 5-15% decrease in precipitation with a simultaneous 40-45% increase in evaporation (owing to the rise in air humidity
515 deficit) during this period comparing with the previous ones. During the Allerød, the mean runoff was also less that
516 during the post-LGM or the Oldest Dryas, but the difference is not as significant as for the Bølling, owing to the rising
517 precipitation and decreasing evaporation. The response of different parts of the Volga River basin to climate impacts
518 differed from the response of the entire basin as a whole (Fig. 6).

519 During the high-flow post-LGM and Oldest Dryas periods, the river runoff was mostly formed in the right-bank sub-
520 catchments of the middle Volga: e.g. within the boundary of the modern Oka River basin, the runoff was 70% more
521 than the spatially averaged one for the Volga basin. This result is confirmed by the data of a paleogeographic
522 reconstruction of the runoff of ancient channels, most of the traces of which are located on the right bank of the middle
523 Volga. On the contrary, on the catchment areas of the Upper Volga and the left-bank part of the middle Volga (Kama
524 basin), the river runoff is estimated to be 30-40% less than the average value for the basin.

525 According to the simulation results, significant changes occurred in the intra-annual flow regime of the Volga in
526 comparison with the modern regime. In the modern climate, the high flow season runs from April to June and makes
527 up 54% of the annual runoff. In the considered paleo-periods, the high-flow season was a month later (from May to
528 July), and the share of the annual runoff for these months varied from 75% to 85% with the largest value in the Oldest
529 Dryas (Fig. 7). The simulated runoff from the sub-basins of the Oka and Kama Rivers, as well as from the Upper
530 Volga was generally characterized by the same tendencies as for the runoff from the whole Volga.



532

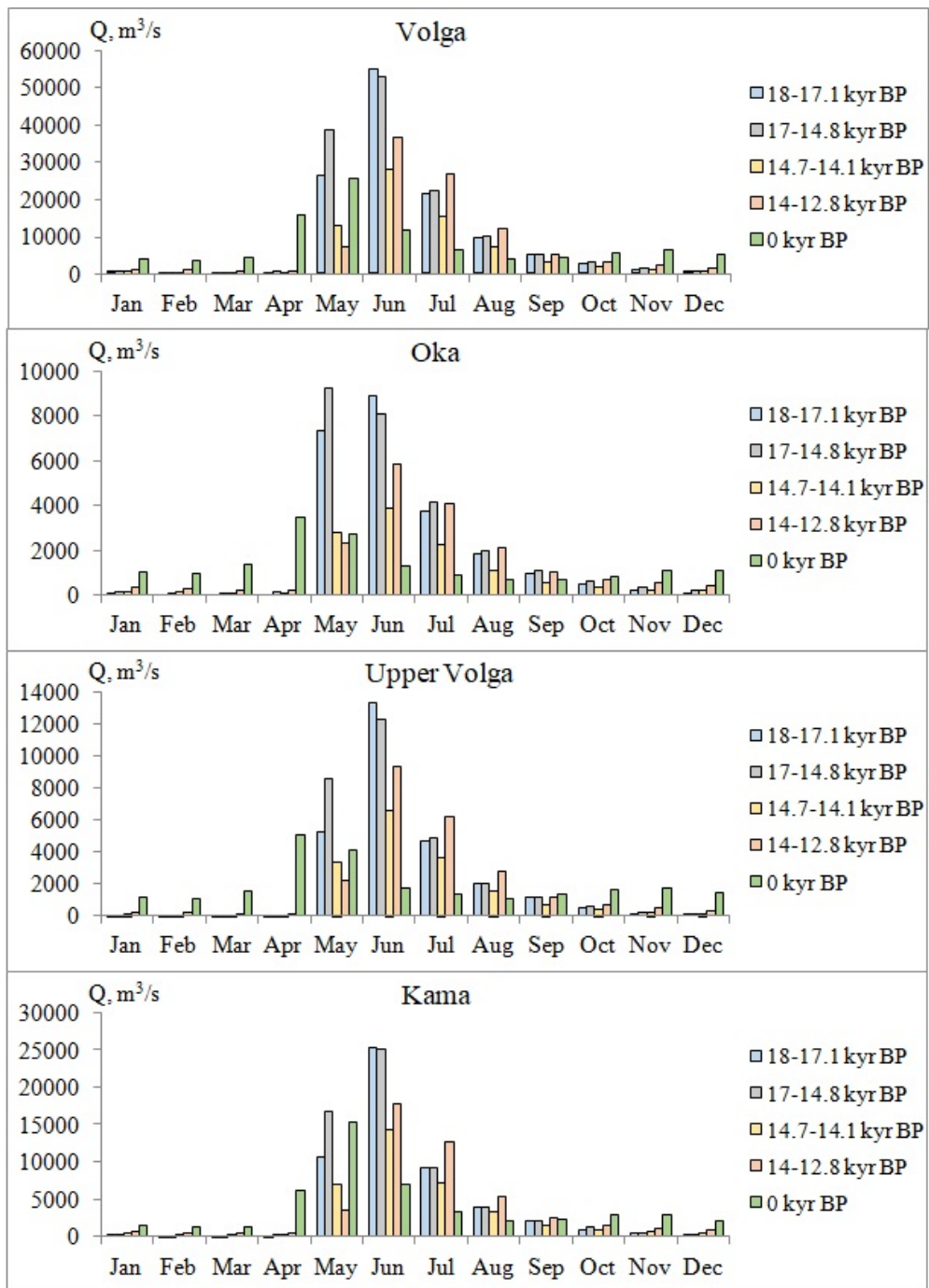
533

534

535

536

Figure 6: The mean annual runoff simulated for different periods of deglaciation and for the modern climate. Top to down: the entire Volga basin, the Oka River Basin (right-bank part of the middle Volga), upper part of the basin, the Kama River Basin (left-bank part of the middle Volga).



537

538 **Figure 7: The mean monthly flow simulated for the different periods of deglaciation and for the modern climate. Top to**
 539 **down: the entire Volga basin, the Oka River Basin (right-bank part of the middle Volga), upper part of the basin, the Kama**
 540 **River Basin (left-bank part of the middle Volga).**

541

542 The most notable difference was a significant increase in the Oka freshet during the post-LGM and the Oldest Dryas,
 543 which we explained by a larger influence of permafrost together with the increased snow water equivalent due to an
 544 increased sum of the solid precipitation as mentioned above. The long-term mean of the annual peak discharge at the
 545 outlet of the Volga River during the post-LGM and the Oldest Dryas turned out to be 3 times higher than the
 546 corresponding mean simulated under the modern climate, and reached the values of 100,000 m³/s. The mean maximum
 547 discharge of the Oka River was as much as 4 times higher than the modern value, reaching 21,000 m³/s during the
 548 Oldest Dryas. A significant increase in the mean peak discharge of snowmelt flood compared to the current one was
 549 also obtained for the Upper Volga (3.7 times) and for the Kama (2.5 times). Peak flow makes the greatest contribution
 550 to the re-shaping of river channels, activates sediment flow and processes of transformation of channel forms.

551 According to the hypothesis of Sidorchuk et al. (2021), it was the snowmelt floods that turned out to be the main
552 driver of fluvial activity and the formation of the palaeochannels occurring in the modern Volga basin and formed
553 between 17.5 ka BP and 14 ka BP.

554 Our results do not contradict this hypothesis, since the largest increase in the simulated mean peak flow occurred in
555 the Volga basin during the Oldest Dryas period (17-14.8 kyr BP).

556 Thus, we summarized that, according to the data of paleoclimate modeling, the climate of the Volga basin in the period
557 from 18 kyr BP to the end of the Oldest Dryas (14.8 kyr BP) was characterized by low air temperature (11-13°C less
558 than in the modern climate) and low precipitation (24-32% less than in the modern climate). At the same time,
559 according to our experiments with the hydrological model, the mean annual Volga runoff during the Oldest Dryas
560 (17-14.8 kyr BP) could reach up to 360 km³, which is almost 40% higher than the modern runoff, and the mean annual
561 peak flow could increase 3 times. The main factors of the increased runoff were a decrease in evaporation from the
562 Volga paleo-catchment as well as the spread of permafrost reducing runoff losses due to infiltration into soils, which
563 all together compensated, over and above, for the decrease in precipitation.

564 Note that the significant hydrological role of permafrost in the considered paleoperiod could be significantly less in
565 the process of its degradation in later periods. This can be evidenced, in particular, by the end of increased flow shortly
566 after 14 ka BP, i.e. in the Allerød, which can hypothetically be associated with thawing of the permafrost by that time.
567 However, the permafrost completely recovered during the Younger Dryas stadial (12.8-11.8 ka BP), but the formation
568 of large palaeochannels did not resume during this period. On the contrary, it was noted above that there is a dip in
569 dates for the 12.5-11.5 ka BP interval, which may indicate a decrease in fluvial activity. This is also supported by the
570 coincidence of this period with a drop in the sea level, the Yenotayevka regression (Makshaev and Tkach, 2023).

571 **5 Conclusions**

572 Our study was aimed at verifying the physical consistency of the hypothesis asserting the hydroclimatic origin of the
573 Early Khvalynian transgression of the Caspian Sea. When *a priori* formulating the hypothesis, we firstly relied on the
574 up-to-date and well-founded OSL-datings (Kurbanov et al., 2021, 2022, 2023; Butuzova et al., 2022; Taratunina et
575 al., 2022), which referred the sea level stage well above +10 m a.s.l. (likely up to +22 ÷ +35 m a.s.l.) to the final period
576 of deglaciation, 17-13 kyr BP. Nowadays, this is the highest dated sea level rise in the Quaternary history of the
577 Caspian Sea, since the maximum stage of the Early Khvalynian transgression (+48+50 m a.s.l.) has still not been dated
578 in any geochronological study. Secondly, we relied on the results of recent (Panin et al., 2020, 2021; Borisova et al.,
579 2021) and earlier (Kalinin et al., 1966; Panin et al., 2005; Sidorchuk et al., 2009) publications, which argued a
580 negligible contribution of meltwater runoff (due to the Scandinavian ice-sheet melting and outflows of ice-dammed
581 proglacial lakes) to the transgression of the sea during the considered, 17-13 kyr BP, period. Thirdly, our hypothesis
582 was based on the ubiquitous presence of large river palaeochannels, whose age was estimated within the close interval,
583 18-13 kyr BP, in the Caspian Sea catchment and adjacent river basins (Borisova et al., 2006; Sidorchuk et al., 2009;
584 Panin et al., 2013, 2017; Panin and Matlakhova, 2015). Herewith, the palaeochannels are located in various parts of
585 the Volga basin, including those completely isolated not only from the last, but also from all Quaternary glaciations,
586 so the glacial meltwater was unlikely to contribute to their formation (Sidorchuk et al., 2009; 2021).

587 Thus, previous studies have given us the reasons to believe that the hypothesis put forward does not contradict the
588 present knowledge on the nature of the Early Khvalynian transgression. That is why we reduced the hypothesis
589 verification to evaluation of its physical feasibility, i.e. the physical feasibility of the CSL rise above +10 m a.s.l. under

590 the climate of the deglaciation period, 17-13 kyr BP, in the absence of visible glacial meltwater effect. We carried out
591 a comprehensive study of the physical consistency of the proposed hypothesis and obtained the following new results:

592 1. Using the coupled ocean and sea-ice general circulation model INMIO COMPASS – CICE driven by the climate
593 model INMCM4.8 in accordance with the PMIP4 and CMIP6 modelling protocols, we estimated the equilibrium water
594 runoff (irrespective of its origin), which could be sufficient to maintain the considered sea level under the modelled
595 effective evaporation from the entire sea surface area. We found that the mean equilibrium runoff into the Caspian
596 Sea for its highest dated transgressive state at +35 m a.s.l. (17-13 kyr BP) should fall within the range of 400-470
597 km³/year. Assuming that the contribution of the Volga River runoff to the total river discharge in that period was close
598 to the modern one (about 80%), we estimated the river runoff from the Volga River basin during the aforementioned
599 period as 320-375 km³/year, i.e. 1.3-1.5 times larger than the present day's annual runoff.

600 2. An extensive ¹⁴C-dating of the activity of palaeochannels located in the valleys of 18 rivers in the Volga basin we
601 conducted, allowed us to narrow down the time frames of the epoch of high river discharge to 17.5-14 ka BP and
602 relate the estimate of the annual Volga runoff magnitude derived earlier from the size of the palaeochannels (420
603 km³/year (Sidorchuk et al., 2021)) to this epoch. Again, the updated time frames are almost identical to the
604 aforementioned modern dating of the main phase of the Early Khvalynian transgression (17-13 ka BP), i.e. the
605 estimates obtained by the independent methods turned out to be very close. Importantly, the estimate of the runoff that
606 formed the studied palaeochannels occurred not far from and higher than the above maximum estimate of the
607 equilibrium runoff: 420 km³/year and 375 km³/year, respectively. That is, the river flow passing through the ancient
608 palaeochannels could maintain the sea level above +10 m a.s.l. under the climate of the considered epoch. As a result,
609 we argued that 17.5-14 ka BP were thousands of years with a huge water inflow capable of maintaining the Caspian
610 Sea level at the maximum dated marks of the Early Khvalynian transgression, and this inflow was not of glacial origin.

611 3. Using an ECOMAG-based hydrological model of the Volga runoff generation forced by paleoclimate data, we
612 analyzed physically consistent mechanisms of an extraordinary high water inflow into the Caspian Sea both in the
613 absence of visible glacial meltwater effect and under the colder and drier climate than the modern one (e.g., during
614 the Oldest Dryas, 17-14.8 kyr BP, the air temperature was 10.9°C colder and precipitation was 24% less than in the
615 modern climate). Nevertheless, our numerical experiments demonstrated that the mean annual Volga runoff during
616 the Oldest Dryas could reach up to 360 km³, which is almost 40% higher than the modern runoff, and the mean annual
617 peak flow could increase 3 times. The main factors of the increased runoff were the spread of permafrost which
618 resulted in a sharp drop in infiltration into the frozen ground and reduced evaporation from the Volga paleo-catchment,
619 which all together compensated, over and above, for the decrease in precipitation. A huge growth of peak flow during
620 the Oldest Dryas, 17-14.8 kyr BP, greatly contributed to the processes of river channel transformation and could have
621 formed the giant channels over the ancient Volga catchment.

622 Thus, our results do not contradict the hypothesis put forward, that the Early Khvalynian transgression of the Caspian
623 Sea could be initiated and maintained solely by hydroclimatic factors within the deglaciation period, 17-13 ka BP.
624 Also, the hypothesis has proven to be physically consistent, since we found a possible cause of the huge inflow into
625 the Caspian Sea in the absence of visible glacial meltwater contribution.

626 **Code/Data availability**

627 Paleoclimate Simulation Datasets related to this paper can be found
628 at https://pure.mpg.de/pubman/faces/ViewItemOverviewPage.jsp?itemId=item_3187396_4, an open-source online
629 data repository hosted at MPG PuRe (Kageyama et al., 2021).

630 **Author contribution**

631 **Alexander Gelfan:** Conceptualization of the study, Methodology of paleo-hydrological study, Writing, Reviewing
632 and Editing; **Andrey Panin:** Methodology of paleochannels dating, Field works; Writing, Reviewing and
633 Editing; **Andrey Kalugin:** Paleo-hydrological simulations, Writing and Editing; **Polina Morozova:** Paleo-climate
634 simulations, Writing; **Vladimir Semenov:** Methodology of assessing equilibrium river inflow into the sea, Writing;
635 **Alexey Sidorchuk:** Methodology of assessing paleochannel flow; **Vadim Ukraintsev:** Paleochannels dating, Field
636 works; **Konstantin Ushakov:** coupled ocean and sea-ice simulations.

637 **Competing interests**

638 The authors declare that they have no known competing financial interests or personal relationships that could have
639 appeared to influence the work reported in this paper.

640 **Acknowledgements**

641 Radiocarbon dating of alluvial deposits and the numerical experiments with the ocean model were financially
642 supported by the Russian Science Foundation (Grant 19-17-00215). Hydrological simulations were designed within
643 the framework of the State Assignment theme № FMWZ-2022-0001. Geomorphological investigations in river
644 floodplain contribute to the State Assignment theme № FMGE-2019-0005.

645 The present work was carried out within the framework of the Panta Rhei Research Initiative of the International
646 Association of Hydrological Sciences (IAHS).

647 **References**

- 648 Arpe, K., and Leroy, S. A.: The Caspian Sea Level forced by the atmospheric circulation, as observed and modelled,
649 *Quaternary international*, 173, 144–152, <https://doi.org/10.1016/j.quaint.2007.03.008>, 2007.
- 650 Arpe, K., Leroy, S. A. G., Lahijani, H., and Khan, V.: Impact of the European Russia drought in 2010 on the Caspian
651 Sea level, *Hydrol. Earth Syst. Sci.*, 16, 19–27, <https://doi.org/10.5194/hess-16-19-2012>, 2012.
- 652 Arpe, K., Tsuang, B. J., Tseng, Y. H., Liu, X. Y., and Leroy, S. A.: Quantification of climatic feedbacks on the Caspian
653 Sea level variability and impacts from the Caspian Sea on the large-scale atmospheric circulation, *Theoretical
654 and Applied Climatology*, 136, 475–488, <https://doi.org/10.1007/s00704-018-2481-x>, 2019.
- 655 Arslanov, K. A., Yanina, T. A., Chepalyga, A. L., Svitoch, A. A., Makshaev, R. R., Maksimov, F. E., Chernov, S. B.,
656 Tertychniy, N. I., and Starikova, A. A.: On the age of the Khvalynian deposits of the Caspian Sea coast according
657 to ^{14}C and $^{230}\text{Th}/^{234}\text{U}$ methods, *Quaternary International*, 409, 81–87,
658 <https://doi.org/10.1016/j.quaint.2015.05.067>, 2016.

- 659 Borisova, O., Konstantinov, E., Utkina, A., Baranov, D., and Panin, A.: On the existence of a large proglacial lake in
660 the Rostov-Kostroma lowland, north-central European Russia, *J. Quat. Sci.*, 37 (8), 1442–1459,
661 <https://doi.org/10.1002/jqs.3454>, 2022.
- 662 Borisova, O., Sidorchuk, A., and Panin, A.: Palaeohydrology of the Seim River basin, Mid-Russian Upland, based on
663 palaeochannel morphology and palynological data, *Catena*, 66 (1), 53–73,
664 <https://doi.org/10.1016/j.catena.2005.07.010>, 2006.
- 665 Borisova, O. K.: Landscape and Climatic Conditions in the Central East European Plain in the last 22 thousand Years:
666 Reconstruction based on Paleobotanical Data, *Water Resour.*, 48, 886–896,
667 <https://doi.org/10.1134/S0097807821060038>, 2021.
- 668 Brierley, C. M., Zhao, A., Harrison, S. P., Braconnot, P., Williams, C. J. R., Thornalley, D. J. R., Shi, X., Peterschmitt,
669 J.-Y., Ohgaito, R., Kaufman, D. S., Kageyama, M., Hargreaves, J. C., Erb, M. P., Emile-Geay, J., D'Agostino,
670 R., Chandan, D., Carré, M., Bartlein, P. J., Zheng, W., Zhang, Z., Zhang, Q., Yang, H., Volodin, E. M., Tomas,
671 R. A., Routson, C., Peltier, W. R., Otto-Bliesner, B., Morozova, P. A., McKay, N. P., Lohmann, G., Legrande,
672 A. N., Guo, C., Cao, J., Brady, E., Annan, J. D., and Abe-Ouchi, A.: Large-scale features and evaluation of the
673 PMIP4-CMIP6 midHolocene simulations, *Clim. Past.*, 16, 1847–1872, [https://doi.org/10.5194/cp-16-1847-](https://doi.org/10.5194/cp-16-1847-2020)
674 2020, 2020.
- 675 Bronk Ramsey, C.: Bayesian analysis of radiocarbon dates, *Radiocarbon*, 51 (1), 337–360,
676 https://doi.org/10.2458/azu_js_rc.51.3494, 2009.
- 677 Butuzova, E. A., Kurbanov, R. N., Taratunina, N. A., Makeev, A. O., Rusakov, A. V., Lebedeva, M. P., Murray, A.
678 S., and Yanina, T. A.: Shedding light on the timing of the largest Late Quaternary transgression of the Caspian
679 Sea, *Quaternary Geochronology*, 73, 101378, <https://doi.org/10.1016/j.quageo.2022.101378>, 2022.
- 680 Chen, J. L., Pekker, T., Wilson, C. R., Tapley, B. D., Kostianoy, A. G., Cretaux, J. F., and Safarov, E. S.: Long-term
681 Caspian Sea level change, *Geophys. Res. Lett.*, 44 (13), 6993–7001, <https://doi.org/10.1002/2017GL073958>,
682 2017.
- 683 Chepalyga, A. L.: Late glacial great flood in the Ponto-Caspian basin, in: *The Black Sea Flood Question: Changes in*
684 *Coastline, Climate, and Human Settlement*, edited by: Yanko-Hombach, V., Gilbert, A.S., Panin, [AN.](#), and
685 Dolukhanov, P.M., Springer, Dordrecht, 119–148, https://doi.org/10.1007/978-1-4020-5302-3_6, 2007.
- 686 Fadeev, R., Ushakov, K., Tolstykh, M., and Ibrayev, R.: Design and development of the SLAV-INMIO-CICE coupled
687 model for seasonal prediction and climate research, *Russian J. Numerical Analysis and Mathematical Modelling*,
688 33 (6), 333–340, <https://doi.org/10.1515/rnam-2018-0028>, 2018.
- 689 Fedorov, P. V.: Stratigraphy of Quaternary sediments and the history of the development of the Caspian Sea, *Proc. of*
690 *the Geological Institute of the Academy of Science of the USSR*, 2 (10), 1–308, 1957 (in Russian).
- 691 Fedorov, P. V. (Ed.): *Pleistocene of the Ponto-Caspian*. Nauka Press, Moscow, 165 pp., 1978 (in Russian).
- 692 Forte A. M., Cowgill E.: Late Cenozoic base-level variations of the Caspian Sea: a review of its history and proposed
693 driving mechanisms, *Palaeogeography, Palaeoclimatology, Palaeoecology*, 386, 392–407,
694 <https://doi.org/10.1016/j.palaeo.2013.05.035>, 2013.
- 695 Frolov A. V. (Ed.): *Modeling of long-term fluctuations of the Caspian Sea level: theory and applications*, GEOS Publ.,
696 Moscow, 174 pp., ISBN 5-89118-298-X, 2003 (in Russian).

- 697 Frolov, A. V.: Dynamic-Stochastic Modeling of the Paleo-Caspian Sea Long-Term Level Variations (14–4 Thousand
698 Years BC), *Water Resour.*, 48, 854–863, <https://doi.org/10.1134/S0097807821060051>, 2021.
- 699 Gelfan, A., Gustafsson, D., Motovilov, Y., Arheimer, B., Kalugin, A., Krylenko, I., and Lavrenov, A.: Climate change
700 impact on the water regime of two great Arctic rivers: Modeling and uncertainty issues, *Clim. Chang.*, 141, 499–
701 515, <https://doi.org/10.1007/s10584-016-1710-5>, 2017.
- 702 Gelfan, A. N., and Kalugin, A. S.: Permafrost in the Caspian Basin as a Possible Trigger of the Late Khvalynian
703 Transgression: Testing Hypothesis Using a Hydrological Model, *Water Resour.*, 48, 831–843,
704 <https://doi.org/10.1134/S0097807821060063>, 2021.
- 705 Golitsyn, G. S., Ratkovich, D. Ya., Fortus, M. I., and Frolov, A. V.: On the present_day rise in the Caspian Sea level,
706 *Water Resour.*, 25 (2), 117–122, 1998.
- 707 Grosswald, M. G., and Kotlyakov, V. M.: The great proglacial drainage system in Northern Eurasia and its significance
708 for inter-regional correlations, in: *Quaternary Period: Paleogeography and Lithology*, edited by: Yanshin, A.L.,
709 Kishinev, Stiintsa, 5–13, 1989 (in Russian).
- 710 Hunke E. C., Lipscomb W. H., Turner A. K., Jeffery N., and Elliott, S.: CICE: the Los Alamos Sea Ice Model
711 Documentation and Software User's Manual Version 5.1, Los Alamos National Laboratory, 2015.
- 712 Ibrayev, R. A., Khabeev, R. N., and Ushakov, K. V.: Eddy-resolving 1/10° model of the World Ocean, *Izv. Atmos.*
713 *Ocean Phys.*, 48, 37–46. <https://doi.org/10.1134/S0001433812010045>, 2012.
- 714 Kageyama, M., Harrison, S. P., Kapsch, M.-L., Lofverstrom, M., Lora, J. M., Mikolajewicz, U., Sherriff-Tadano, S.,
715 Vadsaria, T., Abe-Ouchi, A., Bouttes, N., Chandan, D., Gregoire, L. J., Ivanovic, R. F., Izumi, K., LeGrande, A.
716 N., Lhardy, F., Lohmann, G., Morozova, P. A., Ohgaito, R., Paul, A., Peltier, W. R., Poulsen, C. J., Quiquet, A.,
717 Roche, D. M., Shi, X., Tierney, J. E., Valdes, P. J., Volodin, E., and Zhu, J.: The PMIP4 Last Glacial Maximum
718 experiments: preliminary results and comparison with the PMIP3 simulations, *Clim. Past.*, 17, 1065–1089,
719 <https://doi.org/10.5194/cp-17-1065-2021>, 2021.
- 720 Kakroodi, A. A., Kroonenberg, S. B., Hoogendoorn, R. M., Mohammadkhani, H., Yamani, M., Ghassemi, M. R., and
721 Lahijani, H. A. K.: Rapid Holocene sea-level changes along the Iranian Caspian coast, *Quaternary International*,
722 263, 93–103, <https://doi.org/10.1016/j.quaint.2011.12.021>, 2012.
- 723 Kalinin, G. P., Markov, K. K., and Suetova, I. A.: Fluctuations in the level of the Earth's water bodies in the geological
724 past. Part I, *Oceanology*, 6 (5), 737–746, 1966 (in Russian).
- 725 Kalmykov, V. V., Ibrayev, R. A., Kaurkin, M. N., and Ushakov, K. V.: Compact Modeling Framework v3.0 for high-
726 resolution global ocean-ice-atmosphere models, *Geosci. Model Dev.*, 11 (10), 3983–3997.
727 <https://doi.org/10.5194/gmd-11-3983-2018>, 2018.
- 728 Kalnitskii, L. Y., Kaurkin, M. N., Ushakov, K. V., and Ibrayev, R. A.: Seasonal Variability of Water and Sea-Ice
729 Circulation in the Arctic Ocean in a High-Resolution Model, *Izv. Atmos. and Ocean. Physics*, 56 (5), 522–533,
730 <https://doi.org/10.1134/S0001433820050060>, 2020.
- 731 Kalugin, A.: Hydrological and meteorological variability in the Volga River basin under global warming by 1.5 and
732 2 degrees, *Climate*, 10 (7), 107, <https://doi.org/10.3390/cli10070107>, 2022.

- 733 Kaplin, P. A., Leontiev, O. K., Parunin, O. B., Rychagov, G. I., and Svitoch, A. A.: On the time of Khvalyn
734 transgressions of the Caspian Sea (according to radiocarbon analyses of mollusk shells), *Doklady Acad. Nauk*
735 *SSSR*, 206(6), 735-740, 1972 (in Russian).
- 736 Kaplin, P. A., Parunin, O. B., Svitoch, A. A., Faustov, S. S., and Shlyukov, A. I.: Some results of studying Pleistocene
737 sediments by methods of nuclear chronology and palaeomagnetism, in: *Noveyshaya tektonika, noveyshiye*
738 *otlozheniya i chelovek*, vol. 4, edited by Kaplin, P.A. MSU Press, Moscow, 156-163, 1973 (in Russian).
- 739 Kapsch, M.-L., Mikolajewicz, U., Ziemer, F., and Schannwell, C.: Ocean response in transient simulations of the last
740 deglaciation dominated by underlying ice-sheet reconstruction and method of meltwater distribution,
741 *Geophysical Research Letters*, 49, e2021GL096767, <https://doi.org/10.1029/2021GL096767>, 2022.
- 742 Kislov, A., and Toropov, P.: East European River runoff and Black Sea and Caspian Sea level changes as simulated
743 within the Paleoclimate Modeling Intercomparison Project, *Quaternary International*, 167, 40–48,
744 <https://doi.org/10.1016/j.quaint.2006.10.005>, 2007.
- 745 Kislov, A. V., Panin, A. V., and Toropov, P.: Current status and palaeostages of the Caspian Sea as a potential
746 evaluation tool for climate model simulations, *Quaternary International*, 345, 48–55,
747 <https://doi.org/10.1016/j.quaint.2014.05.014>, 2014.
- 748 Koriche, S. A., Singarayer, J. S., Cloke, H. L., Valdes, P. J., Wesselingh, F. P., Kroonenberg, S. B., Wickert, A. D.,
749 and Yanina, T. A.: What are the drivers of Caspian Sea level variation during the late Quaternary? *Quaternary*
750 *Science Reviews*, 283, 107457, <https://doi.org/10.1016/j.quascirev.2022.107457>, 2022.
- 751 Krijgsman, W., Tesakov, A., Yanina, T., Lazarev, S., Danukalova, G., Van Baak, C. G. C., Agustí, J., Alçiçek, M. C.,
752 Aliyeva, E., Bista, D., Bruch, A., Büyükmeriç, Y., Bukhsianidze, M., Flecker, R., Frolov, P., Hoyle, T. M.,
753 Jorissen, E. L., Kirscher, U., Koriche, S. A., Kroonenberg, S. B., Lordkipanidze, D., Oms, O., Rausch, L.,
754 Singarayer, J., Stoica, M., van de Velde, S., Titov, V. V., and Wesselingh, F. P.: Quaternary time scales for the
755 Pontocaspian domain: interbasinal connectivity and faunal evolution., *Earth-Sci. Rev.*, 188, 1–40,
756 <https://doi.org/10.1016/j.earscirev.2018.10.013>, 2019.
- 757 Kroonenberg, S. B., Badyukova, E. N., Storms, J. E. A., Ignatov, E. I., and Kasimov, N. S.: A full sea level cycle in
758 65 years: barrier dynamics along Caspian shores, *Sediment. Geol.*, 134, 257–274, [https://doi.org/10.1016/S0037-](https://doi.org/10.1016/S0037-0738(00)00048-8)
759 [0738\(00\)00048-8](https://doi.org/10.1016/S0037-0738(00)00048-8), 2000.
- 760 Kurbanov, R., Murray, A., Thompson, W., Svistunov, M., Taratunina, N., and Yanina, T.: First reliable chronology
761 for the Early Khvalynian Caspian Sea transgression in the Lower Volga River valley, *Boreas*, 50 (1), 134–146,
762 <https://doi.org/10.1111/bor.12478>, 2021.
- 763 Kurbanov, R. N., Buylaert, J.-P., Stevens, T., Taratunina, N. A., Belyaev, V. R., Makeev, A. O., Lebedeva, M. P.,
764 Rusakov, A. V., Solodovnikov, D., Költringer, C., Rogov, V. V., Streletskay, I. D., Murray, A. S., and Yanina,
765 T. A.: A detailed luminescence chronology of the Lower Volga loess-palaeosol sequence at Leninsk, *Quaternary*
766 *Geochronology*, 73, 101376, <https://doi.org/10.1016/j.quageo.2022.101376>, 2022.
- 767 Kurbanov, R. N., Belyaev, V. R., Svistunov, M. I., Butuzova, E. A., Solodovnikov, D. A., Taratunina, N. A., and
768 Yanina, T. A.: New data on the age of the Early Khvalynian transgression of the Caspian Sea, *Izvestiya*
769 *Rossiiskoi Akademii Nauk. Seriya Geograficheskaya*, 87(3), 1, 2023 (in Russian).

- 770 Kvasov, D. D. (Ed.): The Late Quaternary history of large lakes and inland seas of Eastern Europe, Suomalainen
771 tiedeakad., Helsinki, 71 pp, 1979.
- 772 Larsen, E., Kjar, K. H., Demidov, I., Funder, S., Grosfjeld, K., Houmark-Nielsen, M., Jensen, M., Linge, H., and Lysa,
773 A.: Late Pleistocene glacial and lake history of northwestern Russia, *Boreas*, 35, 394–424,
774 <https://doi.org/10.1080/03009480600781958>, 2006.
- 775 Leontiev, O. K.: Evolution of the Caspian shores in the Upper Pliocene and Quaternary period, in: Geomorphological
776 analysis during geological research in the Caspian lowland, edited by: Aristarchova L. B., MSU Press, Moscow,
777 106–140, 1968 (in Russian).
- 778 Leontiev, O. K., Rychagov, G. I., Kaplin, P. A., Svitoch, A. A., Parunin, O. B., and Shlyukov, A. I.: Chronology and
779 palaeogeography of Ponto-Caspian (based on result of radiocarbon dating), *Pleistocene Palaeogeography and*
780 *Sediments of Southern Seas of the USSR*, 26–38, 1977 (in Russian).
- 781 Loveland, T. R., Reed, B. C., Brown, J. F., Ohlen, D. O., Zhu, Z., Yang, L., and Merchant, J. W.: Development of a
782 global land cover characteristics database and IGBP DISCover from 1 km AVHRR data, *International Journal*
783 *of Remote Sensing*, 21 (6–7), 1303–1330, 2000.
- 784 Lyså, A., Jensen, M. A., Larsen, E., Fredin, O. L. A., and Demidov I. N.: Ice-distal landscape and sediment signatures
785 evidencing damming and drainage of large proglacial lakes, NW Russia, *Boreas*, 40 (3), 481–497,
786 <https://doi.org/10.1111/j.1502-3885.2010.00197.x>, 2011.
- 787 Makshaev, R. R.: Paleogeography of the Middle and Lower Volga Region during the Early Khvalynian Transgression
788 of the Caspian Sea, Ph.D. thesis, Lomonosov Moscow State University, Moscow, 160 pp., 2019 (in Russian).
- 789 Makshaev, R. R., and Svitoch, A. A.: Chocolate Clays of the northern Caspian Sea region: distribution, structure, and
790 origin, *Quaternary International*, 409, 44–49, <https://doi.org/10.15356/0435-4281-2015-1-101-112>, 2016.
- 791 Makshaev, R. R., and Tkach, N. T.: Chronology of Khvalynian stage of the Caspian Sea according to radiocarbon
792 dating, *Geomorfologiya i Paleogeografiya*, 54 (1), 37–54 <https://doi.org/10.31857/S0435428123010108>, 2023
793 (in Russian).
- 794 Morozova P. A.: Influence of the Scandinavian Ice Sheet on the climate conditions of the East European Plain
795 according to the numerical modeling data of the project PMIP II, *Ice and Snow*, 54 (1), 113–124,
796 <https://doi.org/10.15356/2076-6734-2014-1-113-124>, 2014 (in Russian).
- 797 Morozova P. A., Ushakov K. V., Semenov V. A., and Volodin E. M.: Water budget of the Caspian Sea in the Last
798 Glacial Maximum by data of experiments with mathematical models, *Water Resour.*, 48 (6), 823–830,
799 <https://doi.org/10.1134/S0097807821060130>, 2021.
- 800 Motovilov, Y.: Hydrological simulation of river basins at different spatial scales: 1. Generalization and averaging
801 algorithms, *Water Resour.*, 43, 429–437, <https://doi.org/10.1134/S0097807816030118>, 2016.
- 802 Motovilov, Y., Gottschalk, L., Engeland, K., and Rodhe, A.: Validation of a distributed hydrological model against
803 spatial observations, *Agric. For. Meteorol.*, 98–99, 257–277, [https://doi.org/10.1016/S0168-1923\(99\)00102-1](https://doi.org/10.1016/S0168-1923(99)00102-1),
804 1999.
- 805 Naderi Beni, A., Lahijani, H., Mousavi Harami, R., Arpe, K., Leroy, S. A. G., Marriner, N., Berberian, M., Andrieu-
806 Ponel, V., Djamali, M., Mahboubi, A., and Reimer, P.J.: Caspian Sea-level changes during the last millennium:

- 807 historical and geological evidence from the south Caspian Sea, *Climate of the Past*, 9 (4), 1645–1665,
808 <https://doi.org/10.5194/cp-9-1645-2013>, 2013.
- 809 Panin, A., Adamiec, G., Buylaert, J.-P., Matlakhova, E., Moska, P., and Novenko, E.: Two Late Pleistocene climate-
810 driven incision/aggradation rhythms in the middle Dnieper River basin, west-central Russian Plain, *Quaternary*
811 *Science Reviews*, 166, 266–288, <https://doi.org/10.1016/j.quascirev.2016.12.002>, 2017.
- 812 Panin, A. V., Astakhov, V. I., Lotsari, E., Komatsu, G., Lang, J., and Winsemann, J.: Middle and Late Quaternary
813 glacial lakeoutburst floods, drainage diversions and reorganization of fluvial systems in northwestern Eurasia,
814 *Earth-Science Reviews*, 201, 103069, <https://doi.org/10.1016/j.earscirev.2019.103069>, 2020.
- 815 Panin, A. V., and Matlakhova, E. Yu.: Fluvial chronology in the East European plain over the last 20 ka and its
816 palaeohydrological implications, *Catena*, 130, 46–61, <https://doi.org/10.1016/j.catena.2014.08.016>, 2015.
- 817 Panin, A. V., and Sidorchuk, A. Ju., Borisova, O. K.: Fluvial processes and river runoff in the Russian Plain in the
818 end of the Late Valdai epoch, in: *Geography Perspectives: to the 100th anniversary of K.K. Markov*, Geogr.
819 Dep. MSU, Moscow, 114–127, 2005 (in Russian).
- 820 Panin, A. V., Sidorchuk, A. Y., and Ukraintsev, V. Y.: The Contribution of Glacial Melt Water to Annual Runoff of
821 River Volga in the Last Glacial Epoch, *Water Resour.*, 48, 877–885,
822 <https://doi.org/10.1134/S0097807821060142>, 2021.
- 823 Panin, A. V., Sidorchuk, A. Yu, and Vlasov, M. V.: High Late Valdai (Vistulian) runoff in the Don River basin,
824 *Izvestiya Rossiiskoi Akademii Nauk. Seriya Geograficheskaya*, 1, 118–129, 2013 (in Russian).
- 825 Panin, A. V., Sorokin, A. N., Bricheva, S. S., Matasov, V. M., Morozov, V. V., Smirnov, A. L., Solodkov, N. N., and
826 Uspenskaia, O. N.: Landscape development history of the Zabolotsky peat bog in the context of initial settlement
827 of the Dubna River lowland (Upper Volga basin), *Vestnik Archeologii, Antropologii i Etnografii*, 2, 85–100.
828 <https://doi.org/10.20874/2071-0437-2022-57-2-7>, 2022.
- 829 Panin, G. N. and Dianskii, N. A.: On the correlation between oscillations of the Caspian Sea level and the North
830 Atlantic climate, *Izvestiya, Atmospheric and Oceanic Physics*, 50 (3), 266–278, [https://doi.org/](https://doi.org/10.1134/S000143381402008X)
831 [10.1134/S000143381402008X](https://doi.org/10.1134/S000143381402008X), 2014.
- 832 Peltier, W. R., Argus, D. F., and Drummond, R.: Space geodesy constrains ice age terminal deglaciation: The global
833 ICE-6G_C (VM5a) model, *J. Geophys. Res. Solid Earth*, 120, 450–487, <https://doi.org/10.1002/2014JB011176>,
834 2015.
- 835 Ratkovich, D. Ya.: Modern variations of the Caspian Sea level, *Water Resour.*, 20 (2), 160–171, 1993.
- 836 Rychagov, G.I.: Late Pleistocene history of the Caspian Sea, in: *Comprehensive studies of the Caspian Sea*, edited by:
837 Leontiev, O.K., Maev, E.G., MSU Press., Moscow, 18–29, 1974 (in Russian).
- 838 Rychagov, G. I. (Ed.): *Pleistocene History of the Caspian Sea*, MSU Press, Moscow, 267 pp., ISBN 5-211-03828-2,
839 1997 (in Russian).
- 840 Semikolennykh, D.V., Kurbanov, R.N., and Yanina, T.A.: Age of the Khvalyn Strait in the Late Pleistocene history
841 of the Manych Depression, *Vestnik Mos. Univ. Seria 5. Geogr.*, 5, 103-112, 2022 (in Russian).

- 842 Sidorchuk, A. Yu., Panin, A. V., and Borisova, O.K.: Climate-induced changes in surface runoff on the North-Eurasian
843 plains during the late glacial and Holocene, *Water Resour.*, 35, 386–396.
844 <https://doi.org/10.1134/S0097807808040027>, 2008.
- 845 Sidorchuk, A. Y., Panin, A. V., and Borisova, O.K.: Morphology of river channels and surface runoff in the Volga
846 River basin (East European Plain) during the Late Glacial period, *Geomorphology*, 113 (3–4), 137–157,
847 <https://doi.org/10.1016/j.geomorph.2009.03.007>, 2009.
- 848 Sidorchuk, A., Panin, A., and Borisova, O.: Surface runoff to the Black Sea from the East European Plain during Last
849 Glacial Maximum–Late Glacial time, in: *Geology and Geoarchaeology of the Black Sea Region: Beyond the*
850 *Flood Hypothesis*, edited by: Buynevich, I., Yanko–Hombach, V., Gilbert, A.S., and Martin, R.E., Geological
851 Society of America Special Paper 473, pp. 1–25, [https://doi.org/10.1130/2011.2473\(01\)](https://doi.org/10.1130/2011.2473(01)), 2011.
- 852 Sidorchuk, A. Y., Ukraintsev, V. Y., and Panin, A. V.: Estimating Annual Volga Runoff in the Late Glacial Epoch
853 from the Size of River Paleochannels, *Water Resour.*, 48, 864–876,
854 <https://doi.org/10.1134/S0097807821060178>, 2021.
- 855 Simakova, A. N.: Evolution of vegetation of the Russian Plain and Western Europe in the Late Neopleistocene-Middle
856 Holocene (33-4.8 thousand years BP) (from palynological data), Ph.D. thesis, Geological Institute of the Russian
857 Academy of Sciences, Moscow, 34 pp., 2008 (in Russian).
- 858 Smith, M., and Riseborough, D.: Climate and the limits of permafrost: A zonal analysis, *Permafrost and Periglacial*
859 *Processes*, 13 (1), 1–15, <https://doi.org/10.1002/ppp.410>, 2002.
- 860 Svitoch, A. A.: Khvalynian transgression of the Caspian Sea was not a result of water overflow from the Siberian
861 proglacial lakes, nor a prototype of the Noachian flood, *Quaternary International*, 197, 115–125,
862 <https://doi.org/10.1016/j.quaint.2008.02.006>, 2009.
- 863 Svitoch, A. A. (Ed.): *The Big Caspian: Structure and History of Development*, MSU Press, Moscow, 270 pp., ISBN
864 978-5-19-010904-7, 2014 (in Russian).
- 865 Svitoch, A. A., and Parunin, O.B.: On the rate of formation of mollusk complexes in ancient Caspian sediments,
866 *Vestnik Mos. Univ. Seria 5. Geogr.*, 3, 41-48, 1973 (in Russian).
- 867 Svitoch, A. A., Parunin, O. B., and Yanina, T. A.: Radiocarbon chronology of the deposits and events of late
868 Pleistocene of the Ponto-Caspian region, in: *Quaternary Geochronology*, edited by: Murzaev, V.E., Puning Ya-
869 M.K., Chichagova, O.A., Nauka, Moscow, pp. 75–82, 1994 (in Russian).
- 870 Svitoch, A. A., Selivanov, A. O., and Yanina, T. A.: *Paleogeographic Events of the Ponto-Caspian and Mediterranean*
871 *Pleistocene*, RASHN, Moscow, pp. 289, 1988 (in Russian).
- 872 Svitoch, A. A., and Yanina, T. A.: On the time of the Khvalyn transgression of the Caspian Sea (based on absolute
873 dating data), in: *Geologo-geomorfologicheskiye issledovaniya Kaspiyskogo morya*, edited by: Voropayev, G.I.,
874 Lebedev, L.I., Leontiev, O.K. MSU Press, Moscow, 156-163, 1983 (in Russian).
- 875 Svitoch, A. A., and Yanina, T. A.: *Quaternary Deposits of the Caspian Sea Coasts*, MSU Press, Moscow, 267 pp.,
876 1997 (in Russian).
- 877 Svitoch, A. A., Yanina, T. A., Novikova, N. G., Sobolev, V. M., and Khomenko, A. A.: *Pleistocene of Manych:*
878 *Questions of Structure and Development*, MSU Press, Moscow, 135 pp., 2010 (in Russian).

- 879 Taratunina, N. A., Buylaert, J. P., Kurbanov, R. N., Yanina, T. A., Makeev, A. O., Lebedeva, M. P., Utkina, A. O.,
880 and Murray, A. S.: Late Quaternary evolution of lower reaches of the Volga River (Raygorod section) based on
881 luminescence dating, *Quaternary Geochronology*, 72, 101369, <https://doi.org/10.1016/j.quageo.2022.101369>,
882 2022.
- 883 Toropov, P. A., and Morozova, P. A.: Evaluation of the Caspian Sea level fluctuations during the Late Pleistocene
884 cryochrome epoch based on the results of the numerical climate modeling, *Vestn. Mosc. Univ. Ser. 5. Geogr.* 2,
885 55–61, 2011 (in Russian).
- 886 Tudryn, A., Leroy, S. A. G., Toucanne, S., Gibert-Brunet, E., Tucholka, P., Lavrushin, Y. A., Dufaure, O., Miska, S.,
887 and Bayon, G.: The Ponto-Caspian basin as a final trap for southeastern Scandinavian Ice-Sheet meltwater,
888 *Quaternary Science Reviews*, 148, 29–43, <https://doi.org/10.1016/j.quascirev.2016.06.019>, 2016.
- 889 Ukraintsev, V. Yu.: Evidences of the high river runoff in the river valleys of the Volga basin during the Late Glacial,
890 *Geomorfologiya*, 53 (1), <https://doi.org/10.31857/S0435428122010126>, 2022.
- 891 Ushakov, K. V. and Ibrayev, R. A.: Assessment of mean world ocean meridional heat transport characteristics by a
892 high-resolution model, *Russ. J. Earth. Sci.*, 18, ES1004, <https://doi.org/10.2205/2018ES000616>, 2018.
- 893 Varuschenko, S. I., Varuschenko, A. N., and Klige, R. K. (Eds.): Changes in the Regime of the Caspian Sea and
894 Closed Basins in Paleotime, Nauka, Moscow, 239 pp., 1987 (in Russian).
- 895 Volodin, E. M., Mortikov, E. V., Kostykin, S. V., Galin, V. Y., Lykossov, V. N., Gritsun, A. S., Diansky, N. A.,
896 Gusev, A. V., Iakovlev, N. G., Shestakova, A. A., and Emelina, S. V.: Simulation of the modern climate using
897 the INMCM48 climate model, *Russ. J. Numer. Anal. Math. Modelling*, 33 (6), 367–374,
898 <https://doi.org/10.1515/rnam-2018-0032>, 2018.
- 899 Water balance and level fluctuations of the Caspian Sea. Modeling and prediction, (Ed. V. Gruzinov). Moscow,
900 Rosgidromet. 375 pp, ISBN 978-5-9908623-0-2, 2016 (in Russian).
- 901 Yanina, T. A.: Correlation of the Late Pleistocene paleogeographical events of the Caspian Sea and Russian plain,
902 *Quaternary International*, 271, 120–129, <https://doi.org/10.1016/j.quaint.2012.06.003>, 2012.
- 903 Yanina, T., Sorokin, V., Bezrodnykh, Y., and Romanyuk, B.: Late Pleistocene climatic events reflected in the Caspian
904 Sea geological history (based on drilling data), *Quaternary International*, 465 (4), 130–141,
905 <https://doi.org/10.1016/j.quaint.2017.08.003>, 2018.
- 906 Yanko-Hombach, V., and Kislov, A.: Late Pleistocene and Holocene sea-level dynamics in the Caspian and Black
907 seas: Data synthesis and paradoxical interpretations, *Quaternary International*, 465, 63–71,
908 <https://doi.org/10.1016/j.quaint.2017.11.030>, 2018.
- 909 Zekster, I. S.: Groundwater discharge into lakes: a review of recent studies with particular regard to large saline lakes
910 in central Asia, *Int. J. Salt Lake Res.*, 4, 233–249, <https://doi.org/10.1007/BF02001493>, 1995